5-2021

Validation of a Two-Dimensional Clinostat Design to Provide Functional Weightlessness to Custom Gas Exchange Vessels

Collin R. Topolski
Embry-Riddle Aeronautical University, topolskc@my.erau.edu

VALIDATION OF A TWO-DIMENSIONAL CLINOSTAT DESIGN TO PROVIDE FUNCTIONAL WEIGHTLESSNESS TO CUSTOM GAS EXCHANGE VESSELS

by

Collin R. Topolski

A Thesis Submitted to the College of Engineering Department of Mechanical Engineering in Partial Fulfillment of the Requirements for the Degree of Master of Science in Mechanical Engineering

Embry-Riddle Aeronautical University
Daytona Beach, Florida
May 2021

VALIDATION OF A TWO-DIMENSIONAL CLINOSTAT DESIGN TO PROVIDE FUNCTIONAL WEIGHTLESSNESS TO CUSTOM GAS EXCHANGE VESSELS

by

Collin R. Topolski

This thesis was prepared under the direction of the candidate's Thesis Committee Chair, Dr. Eduardo Divo, Professor Department Chair, Daytona Beach Campus, and Thesis Committee Members Dr. Hugo Castillo, Assistant Professor, Daytona Beach Campus, Dr. Karen F. Gaines, Professor and Dean, Daytona Beach Campus, and Dr. Fardin Khalili, Visiting Assistant Professor, Daytona Beach Campus, and has been approved by the Thesis Committee. It was submitted to the Department of Mechanical Engineering in partial fulfillment of the requirements for the degree of Master of Science in Mechanical Engineering

Thesis Review Committee**:**

Eduardo Divo, Ph.D.
Committee Chair

Hugo Castillo, Ph.D.
Committee Member

Karen F. Gaines, Ph.D.
Committee Member

Jean-Michel Dhainaut, Ph.D.
Graduate Program Coordinator,
Mechanical Engineering

Maj Mirmirani, Ph.D.
Dean, College of Engineering

Fardin Khalili, Ph.D.
Committee Member

Eduardo Divo, Ph.D.
Department Chair,
Mechanical Engineering

Christopher Grant, Ph.D.
Associate Vice President of Academics

06/02/2021
Date

Acknowledgements

First, I would like to thank Dr. Karen Gaines for providing invaluable research space, resources, and mentorship. Additionally, I want to thank Dr. Hugo Castillo for taking me under his supervision, teaching me to “live a little”, and always being eager for Thai spicy noodles. I also want to thank Dr. Eduardo Divo and Dr. Fardin Khalili for their support and guidance through this work. Furthermore, I want to thank the NASA Florida Space Grant Consortium for financially assisting me to make my contribution to simulated microgravity research.

I would like to also thank the Physical Sciences Department for providing me the opportunity to work as a chemistry lab teaching assistant throughout my graduate studies. Along with that, I must thank my chemistry supervisor and friend, AJ McGahran who has helped me along my way through listening to my ramblings or giving advice and taught me how to find better deals.

Next, I want to thank my family and friends for giving their support throughout this work. I would like to thank Andy Zamora for being a great friend and always exchanging new ideas. Also, I want to thank Kayla Hollis for constantly pushing me and creating irreplaceable memories with Rava, Iroh, and Azula. Finally, to my parents, Gene and Joanne Topolski, for all the sacrifices they have made to make my dreams possible and their never-ending belief in me. Thank you for everything.

Abstract

Researcher: Collin R. Topolski

Title: Validation of a Two-Dimensional Clinostat Design to Provide Functional Weightlessness to Custom Gas Exchange Vessels

Institution: Embry-Riddle Aeronautical University

Degree: Master of Science in Mechanical Engineering

Year: 2021

Understanding the impacts of microgravity on bacteria is vital for successful long duration space missions. In this environment, bacteria have been shown to become more virulent, more resistant to antibiotics and form more biofilms. To learn more about these phenomena, many experiments must be sent to the International Space Station, which is cost- and time prohibitive. Instead, the use of ground-based analogs is advantageous to define preliminary results that can later be verified with a space-based experiment. This research explored the development of an innovative 2D clinostat for simulating microgravity using bacteria. Computational fluid dynamics, standards established by previous literature and biological test methods were utilized to validate the system's functionality. More specifically, biological validation consisted of optical density, biofilm analysis and gene regulation. Additionally, prototype vessels were created to utilize aerobic bacteria on future clinostat experiments.

Table of Contents

Page

List of Tables

Page

Table

List of Figures

Page

Figure

Abbreviations

2D	Two-Dimensional
3D	Three-Dimensional
ABS	Acrylonitrile Butadiene Styrene
Ca-Sp	Calcium Spirulan
CAD	Computer-Aided Design
CFD	Computational Fluid Dynamics
CFU	Colony Forming Unit
ECLSS	Environmental Control and Life Support System
ESA	European Space Agency
HARV	High Aspect Ratio Vessel
ISRU	In-Situ Resource Utilization
ISS	International Space Station
LSS	Life Support System
MELiSSA	Micro-Ecological Life Support System Alternative
NASA	National Aeronautics and Space Administration
NB	Nutrient Broth
PCB	Printed Circuit Board
PWM	Pulse Width Modulation
RCCS	Rotary Cell Culture System
RPM	Revolutions Per Minute
RWV	Rotating Wall Vessel

Nomenclature

ρ_{media}	Density of media
ρ_{cell}	Density of bacteria
μ	Viscosity of media
η	Density of media
ω	Rotational velocity
m	Mass of bacteria
v_{sed}	Sedimentation velocity
V_{cell}	Volume of bacteria
k_B	Boltzmann Constant
D	Diffusion Rate
g	Earth's gravity
a_c	Centrifugal Acceleration
r	Radius from rotation axis to center of vessel
R	Radius from rotation axis to far wall
T	Temperature
t	Time
V_{ref}	Reference Voltage

1. Introduction

With the future of long duration spaceflight missions looking to expand from the International Space Station (ISS) to deep space; specifically, the Moon and Mars, it must be ensured that all critical systems are thoroughly developed before humans begin the extended voyage. One key system that could be greatly improved to account for these longer missions is the Life Support System (LSS) component to remove the reliance of these missions on Earth (Eckart, 1996). Organizations such as the National Aeronautics and Space Administration (NASA) and the European Space Agency (ESA) have developed programs to create a closed loop Environmental Control and Life Support System (ECLSS) (Hendrickx et al., 2006; Jones et al., 2016). The intention for these programs is to incorporate plants and bacteria into the LSS to use waste products generated from the crew and provide a source of nutrition. Additionally, it would be ideal if these organisms could incorporate In-Situ Resource Utilization (ISRU) methods which could make use of the resources available at either the Moon or Mars (Eckart, 1996).

One of the microorganisms that has been selected as a viable candidate in this process is a cyanobacteria named *Arthrospira platensis* (Hendrickx et al., 2006). *A. platensis*, commercially known as Spirulina, is a great source for vitamins (e.g., most B vitamins) and minerals (e.g., Potassium, Iron and Magnesium) (Dillon, Phuc & Dubacq, 1995; Capelli & Cysewski, 2010). Beyond these, clinical trials have found that *A. platensis* can be consumed to protect against cancer, improve the cardiovascular system, and as an anti-viral (Capelli & Cysewski, 2010). *A. platensis* is also beneficial within an ECLSS due to its photosynthetic capabilities. The microorganism can remove carbon dioxide in the air through fixation into biomass while simultaneously providing a supply

of oxygen (Hendrickx et al., 2006), reducing the amount of electrolysis required to maintain the needed amount of oxygen.

This bacterium has seen limited research in space, with the most recent being conducted by the ESA's Micro-Ecological Life Support System Alternative (MELiSSA) program. Sent to the ISS in 2017, the experiment faced technical issues that prevented the researchers for describing effects of microgravity on growth. However, it was determined that, in space, the microorganism could maintain a similar oxygen production rate to controls (Poughon et al., 2020). This was the first experiment to use a bioreactor for cyanobacteria in space so comparison to literature cannot be directly completed. Additionally, another issue with *A. platensis* research is the time to complete the logarithmic growth phase. For this past experiment, the log phase continued for up to a week (Poughon et al., 2020). Photosythentic bacteria, such as *A. platensis*, require extensive experimental durations lasting several weeks to determine any potential changes in growth and physiology which can pose a time constraint issue (Dineshkumar, Narendran & Sampathkumar, 2015).

Instead, *E. coli* is a more appropriate model for understanding the effects of microgravity on bacteria and has been implemented in research using both ground analogs and in space. This specie completes its growth curve within 24 hours under optimal environmental conditions and it easily adapts to different carbon sources and electron acceptors. In microgravity experiments, *E. coli* has shown a shortened lag phase, increasing the final cell concentrations when compared to controls (Klaus, Luttges & Stodieck, 1994; Klaus et al., 1997; Kacena et al., 1999). However, results can vary based on the strain, media usage or from oxygen availability so separate experiments may not

be directly comparable (Calhoun et al., 1993; Ratiu et al., 2017). Another characteristic is is that *E. coli* is found naturally in the human intestine and it is currently the subject of intense study for its various roles in immune response regulation and nutrients and metabolites synthesis (Patnaik & Liao, 1994; Rice et al., 2005; Idalia & Bernardo, 2017). Additionally, some pathogenic strains have the capacity to form biofilms on the internal surfaces of spacecraft units and pose a potential health risk to the crew as research has shown the potential increase in pathogenicity for some strains and other related enteric bacteria (Storrs-Mabilat, 2001; Nickerson et al., 2004; Wilson et al., 2007). Bacteria are unavoidable companions in space missions, both intentionally and unintentionally, and they can exert an important role on their success, so it is imperative to fully understand how bacteria will be affected by microgravity. However, the ability to conduct experiments in a true microgravity environment is limited to the International Space Station (ISS), suborbital or parabolic flights, and drop towers. Both flight options and drop towers only provide microgravity ranging from seconds up to four minutes which is too short to recognize any biological effects (Thomas, Prasad & Reddy, 2000; Wagner, Charles & Cuttino, 2009). Meanwhile, experiments sent to the ISS are costly and generally limited in resources and astronaut intervention (Herranz et al., 2013; Lynch et al. 2006). Alternate methods for simulating microgravity become necessary to accommodate bacteria research.

Microgavity simulation devices, such as clinostats, rotating wall vessels (RWV), and random positioning machines are widely used for a variety of biological models. All three options rotate samples (e.g., plants or microorganisms) around a device-dependent number of axes ranging from one to three (Klaus, 2001). Clinostats grow bacteria under

simulated microgravity conditions if certain criteria are met (Klaus, 2001). The concept behind the devices is that the vessel containing the bacteria would have to maintain low-shear conditions and rotate at a constant rate over an extended period (Klaus, 2001). While rotating perpendicular to the gravity vector, the treatment group cells will try to sediment due to gravity, but the rotation prevents the cells from completely falling so the cell maintains a very small circular sedimentation path in the media (Klaus, Todd & Schatz, 1998; Klaus, 2001). Alternatively, the control group rotates parallel to the gravity vector.

Statement of the Problem

Bacteria experiments generally rely on a high number of replicates to represent different growth phases in a biologically and statistically meaningful way. The commercially available analogs are limited in terms of sample quantity they can treat simultaneously without interrupting the overall experiment. For example, the Rotary Cell Culture System (RCCS), a widely used device allows up to four samples, with volumes varying from 1 to 50 mL, to be treated under a single condition (treatment or control) at the same time. A typical bacterial experiment exploring the effects of microgravity on growth dynamics would require a minimum of 8 samples per treatment to represent the different sections of a growth curve.

Purpose Statement

This study has two main purposes: 1) to design and construct a prototype “high throughput” two-dimensional (2D) clinostat specific for bacterial studies, and 2) to

validate its ability to induce physiological and transcriptional regulation of bacterial populations grown under a simulated microgravity environment. Specifically, our prototype was subjected to criterion established from previous literature, compared to an industry standard device (RCCS, Synthecon) and modeled with Computational Fluid Dynamics software (Klaus et al., 1997). A secondary objective was to design a prototype for a growth vessel that provides varying degrees of gas diffusion for future experiments with strict aerobic and microaerophilic bacteria, such as cyanobacteria, on our clinostat.

Research Questions

1. Does our prototype clinostat provide an environment suitable for exposing cells to simulated microgravity?
2. How can we validate, biologically, simulated microgravity-induced physiological and transcriptional changes?
3. How does the clinostat compare to an industry standard device?

2. Review of the Relevant Literature

This chapter provides previous literature was necessary to complete this work. It describes two organisms that are necessary to understanding the effects of microgravity on. Additionally, the functionality and theoretical background of microgravity analogs in relation to bacteria is discussed in depth.

2.1 The Utility of *Arthrospira platensis*

The use of *A. platensis* in the human diet originated in an African community where it was served as a dried cake referred to as Dihé (Ciferri, 1983; Ali & Saleh, 2012). Currently, countries around the world have developed mass culturing facilities, such as the United States, China, and Mexico (Ciferri, 1983; Ali & Saleh, 2012). This cyanobacterium has been specifically referred to as being potentially the best food for the future (United Nations World Food Conference, 1974). *A. platensis* is unique in that it lacks cellulose in its cell wall which allows humans to digest the bacteria directly without preprocessing (Dillon, Phuc & Dubacq, 1995).

Beyond the nutritional value, studies have shown that consumption of this cyanobacterium provides anti-cancer, anti-viral, and cardiovascular benefits (Capelli & Cysewski, 2010; Karkos et al., 2011). Specifically, an experiment was conducted in Egypt by Makhlouf & Makhlouf in 2012 where rats were exposed to a cesium-137 source under two conditions: 2 and 4 Gy. This occurred across 45 days. One treatment group of rats were fed *Arthrospira* for 10 days leading up to the experiment. Following the trial, rats who had consumed the microorganism had been found to have a significant reduction of oxidative stress in the liver compared to the rats that were not administered

Arthrospira. This radiation protection effect would be important in for future astronauts for long duration space missions.

Even though *A. platensis* has many apparent nutritional benefits based on the vitamins and minerals that are consumed, there are lesser-known anti-viral advantages to consuming this cyanobacterium. An active extract was discovered called calcium spirulan (Ca-SP) that was applied to multiple viruses, in a lab setting (Hayashi et al., 1996). The viruses looked at were HSV-1, measles, mumps, coxsachie, polio and influenza A viruses (Hayashi et al., 1996). The use of Ca-SP was able to successfully inhibit these viruses from penetrating the host cells (Hayashi et al., 1996). Additionally, another study used mice and provided various daily dosages of a cold-water extract of *A. platensis* and found that this extract could be used to completely inhibit the flu (Chen et al., 2016). The extract was also determined to increase the survival rate compared to the control group (Chen et al., 2016). Another health benefit is the cardiovascular benefits obtained from consuming *A. platensis*. It has been found that consumption of this cyanobacterium can lower blood pressure and cholesterol among also protecting hearts during and recovering from heart attacks (Capelli & Cysewski, 2010).

2.2 *A. platensis* in space

For long duration spaceflight missions, especially to the Moon, Mars, and beyond, it is key for to have a versatile life support system that is as close to a closed loop as possible. Doing so reduces the need for resupply missions which can be very costly. Instead, the system would regenerate or recycle food, air, water, and waste either mechanically or with the help of different organisms. In this case, *A. platensis* contains multiple benefits that should warrant its own bioreactor onboard the spacecraft and or

habitat. The ESA has also become aware of the flexibility of this organism through its MELiSSA program. The purpose of the previously listed project is to work towards a closed loop system where multiple different microorganisms and plants are chosen that could be included with a human crew and need little to no resupply missions (Hendrickx et al., 2006). *A. platensis* was included in the project's research for its ability to fixate carbon dioxide and produce oxygen at high rates as well as an important dietary supplement. Additionally, research has been conducted that replaces the normal nitrogen source used within the growth media with either urea or urine; where the former is isolated from the latter (Feng & Wu, 2006; Sukumaran et al., 2018).

Although this cyanobacterium is a very promising candidate for inclusion in an ECLSS system in space, there have been few studies that have grown *A. platensis* in space. The most recent payload was completed by the MELiSSA Foundation in 2017 and referred to as ArtEMISS (Leys, 2018). The mission lasted for over a month and sought to grow a culture of the microorganism in a bioreactor so that the oxygen produced could be incorporated into the ISS cabin air supply for the astronauts. Upon data analysis, the results for growth rate were unable to be directly tied to microgravity effects whereas the oxygen production rates were deemed to be relatively unaffected by the environment (Poughon et al., 2020). Although this research is needed, using cyanobacteria can increase the experimental timeline compared to other organisms. For the ArtEMISS payload, one week long growth periods were necessary along with specialized bioreactors.

2.3 Experimenting with *Escherichia coli*

A more commonly used bacteria in space-related research is *E. coli*. This bacterium is a model organism for experiments because its genome has been fully sequenced, it reproduces rapidly, and is a facultative aerobe which allows it to use multiple electron acceptors (Idalia & Bernardo, 2017). This microorganism is roughly cylindrical with a typical length of 1 µm and a diameter of 0.35 µm (Idalia & Bernardo, 2017). *Escherichia. coli* can reproduce every 20 minutes and has a standard growth curve lasting 24 hours, in optimal conditions (Tortora, Funke & Case, 2013). This curve is split between four phases (i.e., lag phase, log, stationary, and death phase) as shown in Figure 2.1.

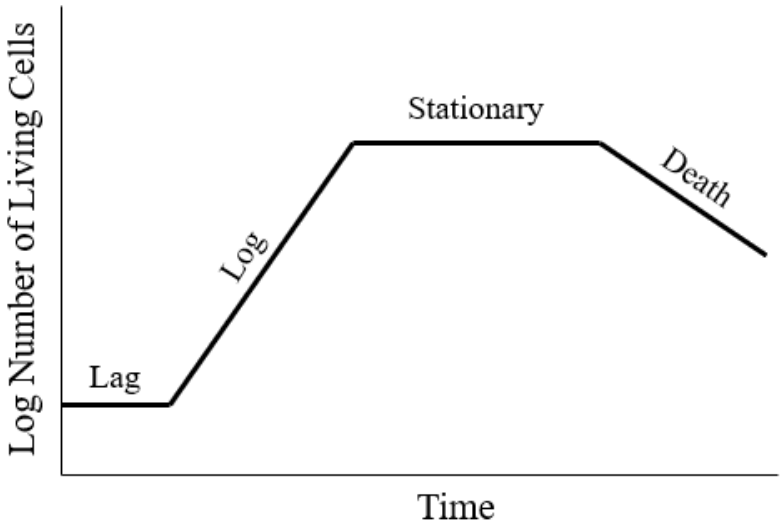

Figure 2.1 General bacterial growth curve

The lag phase begins when an initial culture of cells is transferred into new media and the bacteria begin consuming nutrients in preparation to reproduce (Tortora, Funke & Case, 2013). Once replication begins, the bacterial population expands at an exponential pace until reaching a point of equilibrium; namely, the stationary phase (Tortora, Funke &

Case, 2013). After an extended period, the cells will begin to die off at a logarithmic rate as the available nutrients are exhausted (Tortora, Funke & Case, 2013).

When in suspension, *E. coli* cells typically grow separate from one another. However, when in contact with a surface, *E. coli* will create a sticky biofilm to allow itself to remain adhered to solid surfaces (McLean et al., 2001). Biofilms have been found to become more resistant to environmental stressors (i.e., salt concentration, oxidizers and low pH levels) which can improve their ability to grow in those conditions (Lynch et al., 2006). Additionally, these films are more capable of resisting disinfectants and antibiotics which poses a large issue to astronaut health (McLean et al., 2001; Matin & Lynch, 2005).

2.4 *Escherichia coli* in microgravity

Because of the many reasons to study this bacterium, there have been many studies that have researched the effects of microgravity using *E. coli*. Those studies consist of both ground-based devices and spaceflight payloads. Previous experiments have shown that *E. coli* has a reduced lag phase in true microgravity, which allows the cells to begin proliferating sooner (Thévenet, D'ari & Bouloc, 1996; Klaus et al., 1997; Kacena et al., 1999). The environment also produces a larger final cell population and higher membrane potential which can increase survivability in microgravity conditions (Klaus, Luttges & Stodieck, 1994; Kacena et al., 1999; Vukanti, Mintz & Leff, 2008). These results have also been observed following experiments with ground-based analogs (Brown, 1999; Lynch et al., 2006; Arunasri et al., 2013).

2.4.1 Gene Expression

Understanding the effects of microgravity on *E. coli*, and other bacteria, in relation to altered gene expression is vital not only for bacteria, but also for humans. This is because research using microorganisms with fast reproduction cycles can uncover adaptations necessary for living in reduced gravity conditions (Nickerson et al., 2004). In microgravity, bacteria, including *E. coli*, have been found to alter their gene expression related to virulence, cellular aggregation, biofilm production and general stressors (Wilson et al., 2007; Vukanti, Mintz & Leff, 2008; Zea et al., 2017; Aunins et al., 2018).

A unique aspect of the non-mixed environment during true or simulated microgravity is that the bacteria encounter nutrient depletion zones (Vukanti, Mintz & Leff, 2008). Essentially, without mixing, the cells can only consume nutrients immediately around them and any waste products remain in the same region. Because of this, genes related to nutrient starvation have been shown to be up-regulated (Vukanti, Mintz & Leff, 2008). However, another study was conducted with a simulated microgravity analog that incorporated glycerol which was found to negate the starvation response (Arunasri et al., 2013).

3.4.2 Biofilm Formation

Another important factor with *E. coli* in space-based research is that this bacterium lives in the human intestine (Idalia & Bernardo, 2017). Because of this, all spacecraft will have a high likelihood of *E. coli* colonies forming, among other bacteria, growing in various areas. In both a true and simulated microgravity

experiment, *E. coli* was more prone to not only forming a biofilm, but also for that film to adhere tighter to the surface than controls (McLean et al., 2001; Lynch et al., 2006). In addition to this, these films were more resistant to salt and ethanol, as well as antibiotics (Lynch et al., 2006).

To capture the effects of simulated microgravity on biofilms, the cells were grown on microbeads which were later placed within a microgravity analog (Lynch et al., 2006). However, another method to study biofilms within simulated microgravity is without the use of microbeads. Doing so allows the bacteria to grow in a planktonic state initially while in constant suspension. Once in the log phase, the bacteria may begin forming a biofilm as cells begin to aggregate with one another (Costerton et al., 1995).

Furthermore, biofilm formation in spacecraft can damage or reduce the performance of various systems. Such was the case on the Salyut and Mir spacecraft when hundreds of bacteria, including *E. coli*, were isolated from air, surface, and water sampling (Storrs-Mabilat, 2001). The microbial growth led to destruction of a window, water blockage, and short circuits (Storrs-Mabilat, 2001). Currently, the ISS faces issues with biofilm formation primarily in the water recovery system and they are only kept in control as it is difficult to entirely remove the bacteria (Zea et al., 2020).

2.5 Microgravity Analogs

The best option for microgravity experiments would be on the ISS since the gravity levels are relatively consistent compared to other commercial options (Thomas, Prasad & Reddy, 2000). However, it is not feasible to constantly send every experiment

because of the limited availability of launches, multiple trials necessary to conduct a proper experiment, storage space, and astronaut time (Herranz et al., 2013; Lynch et al. 2006). As an example, researchers must work with a payload integration company to define the experimental constraints which can take up to many weeks. By the time a payload can be launched to the ISS, typically, several months have passed. In some cases, researchers develop hypotheses without preliminary data and must reevaluate the experimental design after the payload is returned. This in turn extends the total time and cost required to obtain a statistically viable experiment. Instead, other methods are needed to test these hypotheses more rapidly.

There are multiple possibilities to provide a true microgravity condition. Two options involve flight: one being a suborbital launch and the other being parabolic airplane flights. The first option has been a newly developing field, commercially, as launch providers such as Blue Origin enable researchers to have roughly four minutes of true space conditions during the rocket capsules suborbital trajectory (Moro-Aguilar, 2014). Alternatively, parabolic flights aim to simulate microgravity in multiple, 30-seconds long, free fall trajectories as the plane adjusts its flight in parabolic motions (Thomas, Prasad & Reddy, 2000; Moro-Aguilar). However, both methods require experiments to experience hyper-g forces as they are accelerated upward which can make defining microgravity effects on organism difficult to separate from the increase in force.

The only microgravity analog capable of providing a true microgravity environment on the ground is free fall from a drop tower (Herranz et al., 2013). This method places an experiment around 150 meters high and then drops the experiment for 5-10 seconds which allows the payload to reach terminal velocity and achieve a

microgravity level of 10^{-5} (Thomas, Prasad & Reddy, 2000). The use of a parabolic flight or a drop tower is beneficial in that many trials can be conducted rather quickly compared to a suborbital flight. Although, cellular physiology will typically take longer than these options to respond to the microgravity environment (Krauss, Bostian & Raab, 2013).

To get past this shortcoming, there are multiple devices that have been designed which rotate a biological sample around one or more axes (Klaus, 2001). The purpose of the rotation is for the sample to not experience gravity in a consistent orientation; doing so will expose the sample to an omni-directional gravity vector (Klaus, 2001). This effect can be representative of microgravity because a sample is not pulled by gravity in a single direction. These devices can incorporate plants or microorganisms at a relatively low cost; however, each device must be designed to accommodate a specific type of organism (Herranz et al., 2013).

One version, known as a random positioning machine, rotates samples around two axes at random intervals which can aid in providing a more accurate depiction of what would occur in microgravity due to removing any rotational bias from a single direction that occurs in the experiment. Instead, a three-dimensional (3D) clinostat maintains the same rotational speed on both axes. These methods are reserved for larger volume samples or containers (Brungs, S, Hauslage & Hemmersbach, 2019). Alternatively, there are 2D clinostats and rotating wall vessels (RWV) that only rotate around a single axis and are recommended for smaller volumes and cells (Brungs, S, Hauslage & Hemmersbach, 2019). The main difference between these two devices is that RWVs promote mixing as well as an inflow of nutrients and outflow of waste (Klaus, 2001).

Instead, the 2D clinostat aims to more closely mimic the fluid conditions in space (Klaus, 2001). Typically, samples are placed along the rotation axis of these devices to reduce the effects of centrifugal acceleration (Klaus, 2001; Brungs, S, Hauslage & Hemmersbach, 2019). The acceleration value, found using Eq. 2.1, is determined based on the worst-case scenario which occurs at the wall of the vessel being used since that radius is furthest from the axis of rotation. When working with bacteria, the vessels must be filled with media so that there is zero headspace (i.e., no bubbles) to provide a low shear environment (Klaus et al., 1997).

Additionally, the relative g force that is experienced during the experiment can be obtained by substituting the system's rotational velocity (Eq. 2.2) into Eq. 2.3 to obtain Eq. 2.4 (Krauss, Bostian & Raab, 2013). To conduct experiments with simulated gravity levels similar to the ISS, the relative g force should be between in the range of 10^{-3} and 10^{-6} (Böhmer & Schleiff, 2019; Herranz et al., 2013).

$$a_c = r\omega^2 \tag{2.1}$$

where a_c is the centrifugal acceleration, r is the maximal radius from the center of rotation, and ω is the angular velocity in radians per second.

$$v = \frac{2\pi r \omega_{RPM}}{60} \tag{2.2}$$

where v is the angular velocity in meters per second and ω_{RPM} is the angular velocity in RPM.

$$\frac{F_c}{g} = \frac{v^2}{g*r} \tag{2.3}$$

where F_c is the centrifugal force and g is Earth's gravity.

$$\frac{Fc}{g} = 1.12 * 10^{-3} * r * {\omega_{RPM}}^2 \tag{2.4}$$

Ensuring that an experiment is providing an appropriate simulated microgravity environment for bacteria requires further calculations. It is vital to understand the bacteria's motion as the largest factor should be Brownian motion. With this being the case, the cells can be said to be in a state of "functional weightlessness" (Klaus et al., 1997). This motion can be found by calculating the bacteria's diffusion rate using Eq. 2.5 and the Stokes radius of a spherical particle (Eq. 2.6) (Klaus et al., 1997). The diffusion distance (Eq. 2.7) can then be found using the time to complete one rotation in seconds (Klaus et al., 1997).

$$D = \frac{k_B * T}{6 * \pi * \mu * s} \tag{2.5}$$

where D is the diffusion rate, k_B is the Boltzmann constant, T is the media temperature, μ is the media viscosity, and s is the Stokes radius.

$$s = \left(\frac{3V_{cell}}{4\pi}\right)^{\frac{1}{3}} \tag{2.6}$$

where V is the volume of the bacteria cell.

$$x = \sqrt{2Dt} \tag{2.7}$$

where x is the diffusion distance and t is the time to complete one rotation.

With the expected diffusion distance known, it must be compared to the communitive forces acting on the cell. These forces are buoyancy, drag, and friction and should equal zero (Eq. 2.9) if they were to entirely cancel each other out (Todd, 1989). Equation 2.10 shows the expanded form of Equation 2.9. By rearranging Eq. 2.10 and plugging in Eq. 2.11 to solve for sedimentation velocity, Equation 2.12 can be solved.

$$F = F_{gravity} - F_{buoancy} - F_{drag} = 0 \tag{2.9}$$

$$0 = m_{cell} * g - \rho_{media} * V_{cell} g - 6\pi\mu r v_{sed} \tag{2.10}$$

Where ρ_{media} is the density of the media, V_{cell} is the bacteria particle's volume, v_{sed} is the bacteria particle's sedimentation velocity and m_{cell} is the mass of the bacteria.

$$m_{cell} = V_{cell} * \rho_{cell} \tag{2.11}$$

where ρ_{cell} is the density of the bacteria.

$$v_{sed} = \frac{2gr^2}{9\eta}(\rho_{cell} - \rho_{media}) \tag{2.12}$$

$$y = v_{sed} * t \tag{2.13}$$

where y is the circumference of the circular sedimentation path and t is the time to complete one rotation.

The sedimentation distance circumference is found by applying Eq. 2.12 in Eq. 2.13 and the time for one rotation. Finally, the diameter of the circular path can be calculated by dividing the answer from Eq. 2.13 by pi. If this diameter value is significantly smaller than the diffusion distance found from Eq. 2.7, the bacteria can be said to be in a state of functional weightlessness (Klaus et al., 1997).

2.5.1 Commercial Options

There are not many commercial options available for selecting a device. One device that has become an industry standard due to numerous studies correlating results with flight-based results, was developed by Synthecon, and is the Rotary Cell Culture System (Lynch et al., 2006). This device operates similarly to a 2D clinostat but is RWV and rotates a sample directly at the rotation axis and supports a volume from 1mL to 50mL using the company's High Aspect Ratio Vessels (HARVs) (*Synthecon*). Since there have been multiple studies that have used this device, it can be utilized to compare growth trends of *E. coli* with the intended 2D clinostat.

Alternatively, a common random positioning machine used in literature is the Desktop RPM from the Dutch Space company and has also been operated as a 2D clinostat (Brungs, S, Hauslage & Hemmersbach, 2019). Otherwise, these devices are developed by the researchers and only the operating conditions are provided which can prevent the ability to validate previous research using the same devices.

4. Methodology

This chapter discusses the design process for the clinostat as well as each of the experiments completed. Multiple tests were conducted to validate the device's ability to provide a simulated microgravity environment for bacteria along with comparison with an industry standard device.

3.1 Microgravity Analog Selection

To successfully grow bacteria in a simulated microgravity environment, a microgravity analog must be chosen to accommodate *A. platensis* and *E. coli* which both have growth curve lasting longer than many of the available analogs. This would make using parabolic or suborbital flights and drop towers impractical to utilize as these options only provide seconds to minutes of exposure to microgravity. Alternatively, random positioning machines do offer plenty of time to complete an experiment. However, this device type adds additional vibrations from the constantly changing direction that can prevent cell growth similar to true microgravity conditions (Brungs, Hauslage & Hemmersbach, 2019).

This left the clinostat and RWV which function similarly in that they are both rotating about only one axis. The RCCS can only handle four samples at a time and in one orientation which means only a treatment or control replicate can be completed individually. This quickly requires many separate experiments to obtain statistically significant results. For these reasons, it was decided to create a 2D clinostat with additional capabilities that would prove more beneficial than using an RWV.

The intended clinostat would be able to complete an entire experiment, treatment and control, with sample replicates on a single unit by hosting 20 growth tubes in each

group. Additionally, this custom design could accept different attachments to enable the use of any desired vessel. Of particular interest was a vessel for aerobic microorganisms. Since the RCCS has been validated in previous research it was used to compare results with the clinostat design.

3.2 Development of a 2D Clinostat

This section explains the process taken to create the unique clinostat design. Theoretical calculations were used to define system constraints and a series of tests were completed to select the materials needed.

3.2.1 Preliminary Device

While initially learning about 2D clinostats, a prototype device was quickly developed to understand the physical aspects for designing the system. This unit, shown in Figure 3.1, consisted of a 12V DC motor, Pulse Width Modulating (PWM) circuit, potentiometer, and hall effect senor with an output LED screen. This system also used screws to secure Eppendorf tubes at radii between three and five cm. The preliminary version was unable to maintain speeds lower than 130 RPM, which caused too high of centrifugal acceleration. Another issue that was determined was the PWM and potentiometer as the input could only be manually dialed between a minimum and maximum current value by the user rather than being set to a specific RPM.

The radii distribution was placed away from the axis of rotation to allow maximum sample throughput to accelerate experimental discovery. A desired

radius of five centimeters was chosen to increase sample quantity and still provide an adequate environment (Krauss, Bostian & Raab, 2013).

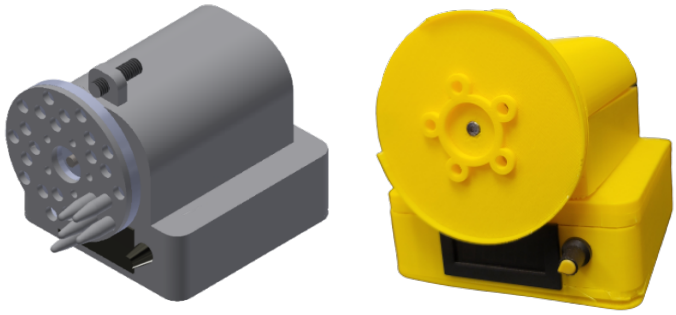

Figure 3.1 A CAD model of the prototype clinostat (left) compared to the 3D printed version (right).

3.2.2 Theoretical Calculations

The clinostat's operating conditions needed to satisfy multiple requirements that previous literature has determined for a low shear simulated microgravity environment. Along with those requirements, a previous experiment using an RCCS (Lynch et al. 2006) as well as the current RCCS configuration were compared to two stepper motors used on the clinostat.

First, the centrifugal acceleration and the relative gravity force experienced was found using equations 2.1 and 2.4. Table 3.1 provides these values along with the percentage of centrifugal acceleration compared to Earth's gravity. Table 3.2 provides the attributes used to represent *E. coli* and the media which was assumed to be water. These values were based on previous research and used equation 2.6 for the Stokes radius of *E. coli* (Klaus et al., 1997).

Table 3.1 Parameters used by the RCCS and Clinostat during experiments.

	RCCS		Clinostat	
	Lynch et al., 2006	Experimental	Without Gearbox	With Gearbox
Rotation Speed [RPM]	25	25	20	8
Rotation Speed [$\frac{rad}{s}$]	2.617	2.617	2.093	0.837
Maximum Radius [m]	0.05	0.0143	0.054	0.054
Centrifugal Acceleration [$\frac{m}{s^2}$]	0.342	0.098	0.237	0.038
Percentage of Earth's Gravity	3.490%	0.998%	2.412%	0.386%
Effective Gravity [$\frac{m}{s^2}$]	0.0350	0.0100	0.0242	0.0039

Table 3.2 Material Properties used for *E. coli* and Media (Klaus et al., 1997; Mika et al., 2016).

Bacteria (*E. coli*)		**Media (Water)**	
Viscosity [$\frac{kg}{ms}$]	0.95	Viscosity [$\frac{kg}{ms}$]	0.001003
Cell Volume [m^3]	1.00E-18	Temperature [K]	300
Stokes Radius [m]	6.20E-07	Density [$\frac{kg}{m^3}$]	1000
Density [$\frac{kg}{m^3}$]	1080		
Mass [kg]	1.08E-15		

Using equations 2.5, 2.7, 2.12 and 2.13 along with information from the previous two tables Table 3.3 was produced. The conditions for all four experiments are well within the means state the bacteria experience functional weightlessness since all sedimentation related movement is significantly smaller than the diffusion from Brownian motion (Klaus et al., 1997).

Table 3.3 Values obtained for expected cellular diffusion for *E. coli*.

	RCCS		Clinostat	
	Lynch et al., 2006	Experimental	Without Gearbox	With Gearbox
Diffusion Rate [$\frac{m^2}{s}$]	3.53E-13			
Diffusion Distance [m]	1.30213E-06		1.45583E-06	2.30187E-06
Sedimentation Velocity [$\frac{m}{s}$]	6.69E-08			
Sedimentation Circumference [m]	1.61E-07		2.01E-07	5.02E-07
Sedimentation Radius [m]	5.11E-08		6.39E-08	1.60E-07
% smaller than diffusion	96%		96%	93%

3.2.3 Updated Design

Iterative designs were created in Autodesk Inventor and SolidWorks computer-aided design (CAD) software. The models were 3D printed using a Qidi X-Pro printer using acrylonitrile butadiene styrene (ABS) material to prevent any possible deformation to occur during experiments in the event of elevated heat. Additionally, the system was adjusted to incorporate a second motor to complete both a control and treatment group simultaneously. This change allowed the clinostat to be capable of holding 20 2mL Eppendorf per group, or 40 total, whereas the RCCS only holds four 4mL vessels in a single orientation.

Figure 3.2 Current clinostat design that is 3D printed and fully assembled.

3.2.4 Component Selection

Motors: Using the initial prototype and the RPM values from the theoretical calculations, a slow rotating DC motor that was capable of rotating at 20 RPM was tested. However, with the low rotation rate, it became apparent that DC motors do not maintain a consistent rotation rate and, instead, oscillate. To overcome this, a stepper motor was selected which could be programmed to complete a rotation consistently and smoothly using micro-steps. Micro-stepping pulses a stepper motor in a way that reduces vibrations and provides a smoother rotation. Additionally, the rotation rate is unaffected by the load applied from holding samples during an experiment if the load remains lower than the rating of the motor. The first stepper motor had 59 Ncm of torque but would vibrate intensely at RPMs below 15. Instead, a 5:1 gearbox was used on the motor which allows for rotation as low as 5 RPM with minimal vibration. The expected loading on each motor would be approximately the mass of twenty 2mL Eppendorf tubes filled with water. The roughly 40g mass at a radius of 5cm multiplied together along with acceleration due to gravity provides a value of 1.962Ncm which is significantly below the motor rating.

Electronics Bay: The clinostat was controlled by an Arduino that operated an OLED display and a rotary encoder in addition to the motors. The display provided the RPM of the motors while the rotary encoder allowed the user to adjust the rotation rate. Stepper motors require a motor driver to process the Arduino commands while also supplying the correct voltage. Each motor was

operated by its own DRV8825 motor controller and programmed to function in 1/32 micro-step mode. These units were more than capable of handling the voltage and current requirements as they can accept up to 45V and pass up to 2.2A per phase. Each DRV8825 driver has an adjustable current output potentiometer which had to be modified before integrating into the final circuit. The adjustment was made based on the rated current of the stepper motors which was 1.68A. Using a multi-meter, the reference voltage (V_{ref}) was changed to reflect half the rated current or 0.84V, in this case. However, because this rated current is the maximum value to operate the motors, the V_{ref} was lowered by roughly 10% on each unit to prevent motor damage.

Power Supply: Powering the circuit required both 5V and 12V for the Arduino and stepper motors, respectively. A 12V power supply unit (PSU) was necessary along with a voltage regulator. The maximum current from the PSU would need to be greater than the operating current needed to power each of the components. Table 3.4 shows the breakdown of each component with its operating current. To accommodate the existing system and any future adjustments, a 12V PSU with up to 10A current was chosen. The Arduino only requires 5V so a L7805 voltage regulator was chosen since it allows for up to 1.5A current draw which exceeds the 0.7A needed for the Arduino and accessories.

Table 3.4 Maximum current usage for each component.

	Max Current (A)
Motors with Drivers	3.36
OLED Screen	0.012
Rotary Encoder	0.03
Fan	0.15
Arduino	0.5
Total	4.052

3.2.5 Circuit Development

The circuit design was first created using a full Arduino and breadboard, see Figure 3.3. This was followed by a completely hand-soldered version, to demonstrate that the system could function with only the ATmega238P chip rather than an entire Arduino. Removing the Arduino greatly reduced the electronics bay footprint within the clinostat from 8.5 x 5.6 x 3.5 cm to 6.4 x 5.5 x 2.2 cm. This change also allowed for all components to be plugged into the same circuit board.

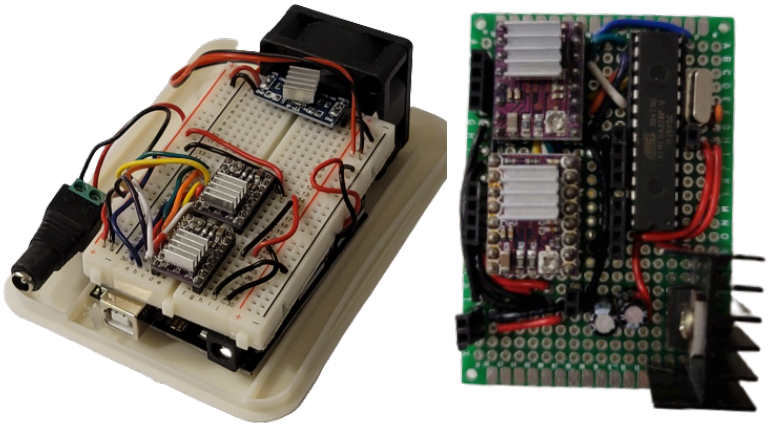

Figure 3.3 Circuit powering early clinostat version consisting of an Arduino and a breadboard (left). The right is a soldered circuit board which reduced the overall footprint while making connections easier.

Rather than produce multiple boards by hand, which involved many hours of work, a printed circuit board (PCB) design was created using Autodesk Eagle. The design was sent to JLCPCB and upon completion, the boards could be assembled within an hour. The Eagle file image compared to the finished boards is shown in Figure 3.4.

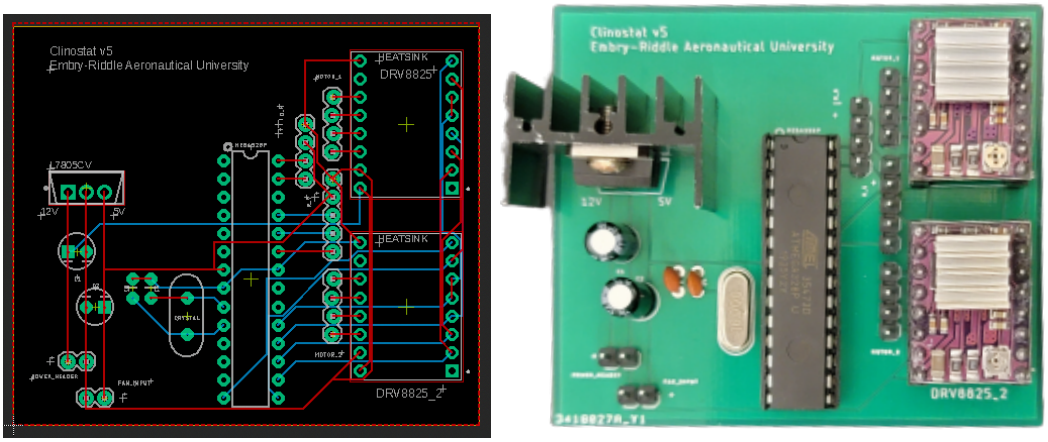

Figure 3.4 The PCB design (left) compared with the assembled board (right).

The only issue faced with these PCBs was the positive 12V power trace connecting to the motor controllers had broken after around 30 minutes of use. Trace breaks can occur from a current larger than the trace width safely allows for. To overcome this issue without having to order new boards, a wire can be soldered along each 12V trace to prevent future breaks.

3.2.6 Vessel Options

Two types of Eppendorf tubes were used to contain samples during clinostat rotation. Both were 2mL volumes with one having a flip cap design and the other had a screw cap, see Figure 3.5. The containers were required to be

absent of any free-moving bubbles to ensure a low-shear environment. The flip cap protruded into the tube when closed which made closing the vessel without any air bubbles difficult. Alternatively, the screw cap did not protrude which allowed the tube to be filled and closed with minimal issues. Additionally, these tubes do not have a gas exchange membrane, therefore *Escherichia coli* was utilized for the experiments since the bacteria does not need oxygen. However, to enable future experiments with aerobic bacteria, such as *A. platensis,* prototype vessels were created that could be placed on the clinostat.

Figure 3.5 The flip cap tube (left) and the screw cap (right) used during experiments.

A volume of 2mL was desired for the prototype vessels and, with autoclavable tubing that had an 12mm inner diameter, 1.66cm long pieces were cut to accommodate the volume. End caps were 3D printed to press-fit onto the ends of the tube pieces while also sitting over a gas permeable membrane. These pieces were all sterilized before assembly using 90% ethanol for 24 hours. The membrane used was a Breathe-Easy Sealing Membrane which is typically used for 96-well plates and is shipped sterilized. The membrane was cut into pieces to fit over the ends of the tube.

Two groups of two samples were created to examine the growth difference of *E. coli* with and without the membrane. A third group consisted of only the

nutrient media to view any contaminations that may have occurred. Samples were created with a 1% volume fraction with Nutrient Broth (NB) media and placed within an incubator at 30°C for 72 hours before measuring optical density, see Figure 3.6.

Figure 3.6 Prototype vessel in three groups: only media, with gas-exchange membranes and without gas exchange membranes.

3.3 Experimental Clinostat Validation

With the 2D clinostat operational, it was necessary to complete an experiment using the device compared with the RCCS. However, trials for each system were varied slightly to accommodate the difference in vessel quantity. Since the clinostat completes control and treatment groups simultaneously, only two 24-hour periods were necessary. Alternatively, the RCCS trials were completed across four instances: two for control and two for treatment. The clinostat was fitted with seven 2mL Eppendorf tubes per group as opposed to four 4mL HARVs on the RCCS. Sampling occurred based on times provided in Table 3.5 with additional samples taken on the clinostat as the platform held more during the experiment.

Table 3.5 Sampling timepoints taken based on the simulated microgravity analog used.

Sampling Time	RCCS	Clinostat
0	X	X
2	X	X
4	N/A	X
5	X	X
6	N/A	X
7	X	X
8	N/A	X
24	X	X

The experiment was limited by the vessels being different from one another based on the device used. Not only is the volume different but also the RCCS has a gas-exchange membrane which can allow the *E. coli* to grow more rapidly (Tortora, Funke & Case, 2013). However, the growth trend should follow a similar pattern assuming both devices are providing a simulated microgravity environment.

A culture of *E. coli* in 2mL of Nutrient Broth (NB) media was grown for 16 hours at 37°C before beginning a trial. From the dense culture, 0.5mL was transferred to into 49.5 mL of NB and inverted for 10 seconds. Next, 14 2mL tubes or four 4mL HARVs were carefully filled to ensure a bubble-free environment. The vessels were placed on their respective unit in an incubator at an optimal growth temperature of 37°C (Doyle & Schoeni, 1984). At each sampling time, optical density was recorded using a BioTek Synergy LX spectrophotometer at 600 nm. This was completed by placing 200 μL of sample in three wells of a 96 well plate. Next, samples were drop-plated through a seven-fold serial dilution to find the quantity of colony forming units (CFUs) to be used as proxy for the number of viable cells on each conditions. Calculating CFUs allows for the number of cells to be compared to the absorbance readings from optical density. For each

sample, seven 2 mL Eppendorf tubes were initially filled with 900 µL of 1X PBS. Then, 100 µL of sample was placed into the first tube and vortexed for ten seconds followed by transferring 100 µL into the next tube. This was completed until the dilution reached the seventh tube. Dilutions four through seven each had 10 µL placed three times into quarter sections of a petri dish filled with Nutrient Agar. Once the drops had absorbed into the agar, the petri dish was placed upside down into an incubator at 30°C and analyzed after 24 hours.

3.3.1 Biofilms Analysis

A separate clinostat experiment was conducted compare the quantity of biofilms formed during clinostat rotation. This clinostat was operated at 8 RPM at 30°C using the screw cap vessels. Additionally, four biological replicates of *E. coli* were made via four separate streak plates. Each of these biological replicates were then triplicated as technical replicates during clinostat rotation and the biofilm analysis. It was hypothesized that more cells would form biofilms in the gravity condition as they are settling within the tube. Alternatively, the simulated microgravity group which is expected to be in constant suspension should form less biofilm on the tube.

The procedure followed that reported by Chavez-Dozal et al., 2016. After 24 hours on the clinostat, samples were carefully emptied of media which contained any planktonic cells. Then the tubes were rinsed with 1X PBS solution two times two fully remove any non-biofilm cells. A solution of 1% crystal violet was added afterwards and remained for 20 minutes until being removed and rinsed with distilled water three times. The tubes were then filled with 91%

isopropanol and left for another 20 minutes to resuspend the crystal violet and the biofilms associated with it. Optical density was measured at 490nm to obtain the concentration of biofilm.

To determine the residual effects of simulated microgravity on biofilm formation, the planktonic cells that were removed from the tubes were grown for another 24 hours on cell culture plates. One mL aliquots of a 1:100 dilutions in NB were transferred into the wells of a twelve well plate. This plate was placed in a 30°C incubator and the previous procedure involving crystal violet was recompleted to identify the quantity of biofilm formation in the well plate.

3.3.2 Differential Gene Expression

In order to explore the effect of simulated microgravity on the transcriptional regulation in *E. coli*, the procedure to construct RNA libraries in preparation for high-throuput sequencing and transcriptome analysis previously reported by Castillo et al., 2018 was followed, using the cultures directly from the clinostat.

3.4 Utilizing CFD

Ansys Fluent was used to simulate the environment within a screw-cap Eppendorf tube used during a clinostat experiment. From the calculations in a previous section, the clinostat was found to provide an acceptable environment to establish functional weightlessness. Ansys Fluent was used to verify this finding by completing a series of simulations to track the cell concentration of the bacteria while on the clinostat. Three cases defined the operational modes: gravity only (no rotation), simulated microgravity (8

RPM), and rapid rotation (100 RPM). To visualize these phenomena, each case was physically demonstrated with *A. platensis*.

The internal tube environment was modeled as a cylinder with a 40 mm length and an 8 mm diameter. Next, the model was meshed using 30 divisions on each edge of the tube and the element size was initially listed as 0.005 m. The model was later subjected to a mesh independence study to ensure the model was unaffected by the sizing of the elements.

3.4.1 Model Setup

The simulation utilizes bacteria cells and a fluid media, which requires a multiphase model. The model must track granular particles to calculate the distribution of bacteria during the simulation, so the Eulerian model was selected. For the primary phase (media), the properties of water were assumed, and the secondary phase (bacteria) had the properties of *E. coli,* based on previous research; listed prior in Table 3.2 (Klaus et al., 1997; Mika et al., 2016). Both phases were created as fluid materials, with the bacteria having the granular option enabled. The fluid flow was determined to be laminar from the Reynolds equation, Eq 3.1, since Re was below 2300.

$$Re = \frac{\rho_{media} v D}{\mu} = \frac{1 * \frac{8 * 2\pi}{60} * 0.05}{.001003} = 41.76 \quad (3.1)$$

Next, the model was initialized after modifying the starting cell concentration to be 1% or a volume fraction of 0.01 throughout the entire fluid, shown in Figure 3.7. This concentration was initially used during the experimental clinostat experiment.

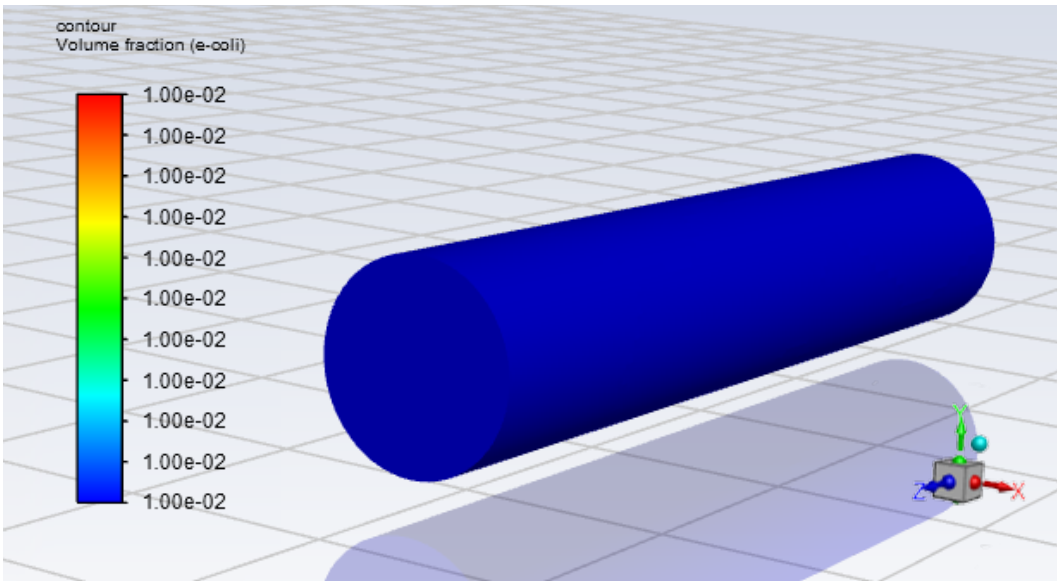

Figure 3.7 Cell concentration of 1% throughout the tube at the beginning of an experiment.

4.4.2 Case 1 - Gravity

The first study completed was with only gravity. If the vessel is stationary, cells will naturally settle and show the concentration of cells largely towards the bottom of the tube. In this case, time steps were not required, and the problem was set to steady-state with gravity of 9.81 $\frac{m}{s^2}$ enabled in the negative y-direction.

4.4.3 Mesh Independence

A mesh independence study was conducted utilizing Fluent's built-in parameterization feature. This was necessary to ensure that each solution provided was not being affected by the mesh being used. The study was completed using the first case, steady state with downward gravity. The area weighted average of the concentration on the front tube wall was recorded on each trial as well as the

volume weighted average concentration over the whole tube. The mesh element size was the independent parameter for each trial with the two averages mentioned, mesh nodes and mesh elements being calculated based on this changing value. The study was iterative to find when altering the mesh would provide a change of less than one percent between trials.

4.4.4 Simulating Rotation

To apply the rotational effects from the clinostat, the position of the tube and the speed must be included in the model. Instead of placing the simulation's reference frame at the center of rotation, it was placed at the center of the tube. This change points the centrifugal acceleration in a constant, positive, y-direction and splits the gravity component into x- and y-components that are functions of cosine and sine, respectively. With gravity enabled in Fluent, Equations 3.2 and 3.3 were entered.

$$X\text{: } 9.81\ [\tfrac{m}{s^2}] * cos(\omega_{RPM} * \tfrac{2\pi}{60} * t) \tag{3.2}$$

$$Y\text{: } \left(\omega_{RPM} * \tfrac{2\pi}{60}\right)^2 * 0.054\ [m] + 9.81\ [\tfrac{m}{s^2}] * sin(\omega_{RPM} * \tfrac{2\pi}{60} * t) \tag{3.3}$$

To test the model using these gravity values, another case can be completed that will show the rotational speed being too high. This would make the centrifugal acceleration become the dominant force and drive a higher concentration of cells at the furthest point from the rotational axis. Since these

equations rely on the simulation time, the model was switched to transient for cases 2 and 3.

These two cases also underwent two trials each where one maintains the initial concentration of bacteria and the second trial includes the growth rate. Since the number of bacteria increases during the experiment, it is possible that the rotation rate may need to be adjusted to maintain the suspended solution. The growth rate used was based on the experimental clinostat experiment and applied as a mass source term which Fluent calls at the beginning of each iteration. The function incorporates the volume fraction of each volumetric mesh cell so that growth can only occur based on the quantity of *E. coli* present in the element.

Additionally, it should be noted that selecting a rotational speed is dependent on the mass of the bacteria used so this would have to be validated for each organism. The experiments completed consist of a maximum duration of 24 hours so that range is used for each simulation to view the simulated cell concentrations after the entire period. This range was inputted as 86,400 seconds and each time step was completed in one second intervals.

4.4.5 Case 2 – Rapid Rotation

To demonstrate the CFD model function in a state where centrifugal force is the dominate force, an RPM of 100 was used. This rotation rate was included in the y-direction's gravity term for centrifugal acceleration. Since the rotational acceleration would be dominate compared to gravity, cells should be pushed against

the furthest radii of the tube which, based on the simulation's reference frame, would be the top of the tube.

4.4.6 Simulated Microgravity

The remaining case for the simulation is to input the 8 RPM that was previously calculated to provide a functionally weightless environment for the cells. Since the RPM and radius selection has been calculated to be maintaining the cell culture in constant suspension, the volume fraction of cells should maintain close to the initial homogeneous distribution. However, due to the rotation, a slight concentration gradient should occur since the centrifugal acceleration is constant in magnitude whereas the gravity vector is rotating.

4. Results and Discussion

This chapter presents the findings to validate the clinostat design. A series of experiments were conducted to determine the validity of the device. These tests dealt with experimental growth, biofilm formation, gene expression, and CFD. Additionally, the prototype vessels are discussed regarding their oxygen availability.

4.1 Experimental growth comparison

Both treatment groups in the Clinostat and RCCS expressed a higher cell density after 24 hours compared to their controls. This aligns with previous research where microgravity has been shown to increase the final cell concentration (Klaus, Luttges & Stodieck, 1994; Kacena et al., 1999; Brown, 1999; Lynch et al., 2006; Arunasri et al., 2013). Additionally, there is nearly three times the cell concentration after 24 hours between the clinostat and RCCS simulated microgravity groups. This variation can be attributed to the difference in the gas exchange capacity of the membrane on the RCCS, compared to our solid microcentrifuge tubes. As a facultative anaerobe, the *E. coli* would have produced energy through fermentation on the tubes used on our clinostat which is known to be less efficient compared to utilizing oxygen (Tortora, Funke & Case, 2013).

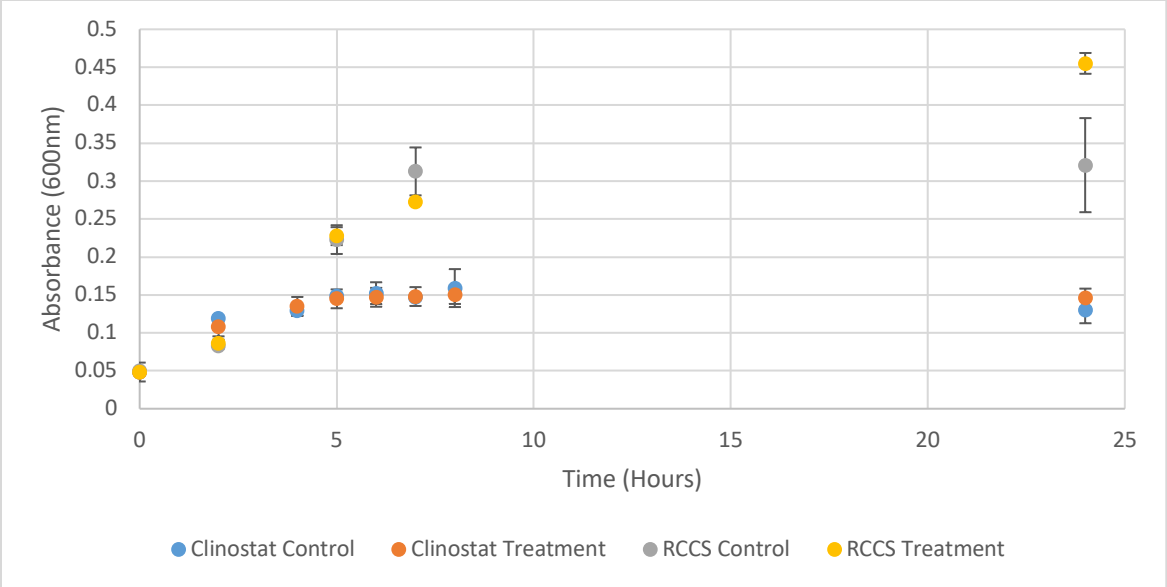

Figure 4.1 Cell concentration based on optical density for both simulated microgravity analogs.

Each sample was drop-plated in addition to an absorbance reading. Figure 4.2 shows the cell count at each time point for the clinostat trials with a linear regression included to provide an estimated growth rate during the exponential phase of the treatment group.

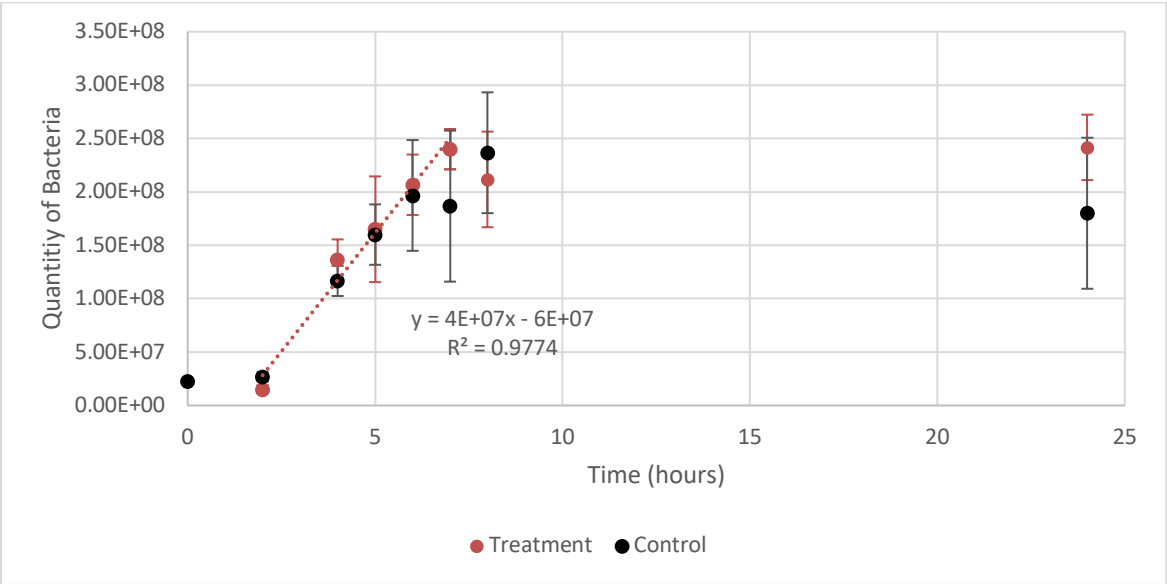

Figure 4.2 Growth curve of *E. coli* for simulated microgravity at 20RPM.

4.2 Biofilm analysis

Following 24 hours on the clinostat at 8 RPM, optical density was recorded and shown in Figure 4.3. Although not significantly greater, the microgravity condition, again, had a slightly higher cell density average. However, because they are not significantly different from one another, the subsequent biofilm analyses were not affected by the total quantity of cells.

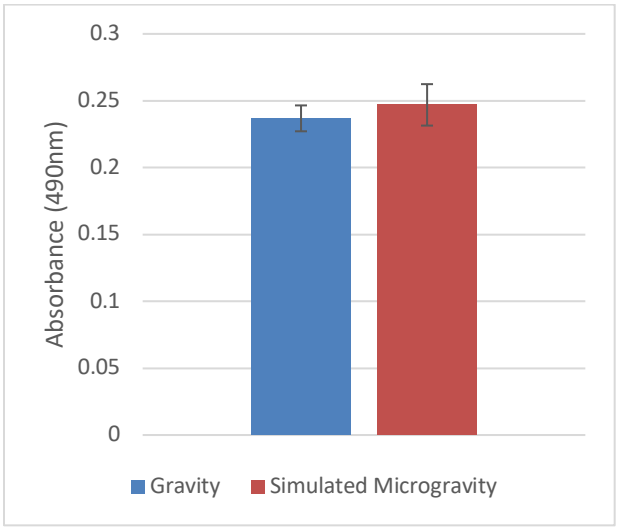

Figure 4.3 Optical density of *E. coli* after 24 hours.

After measuring optical density, the concentration of biofilms on the sample tube walls is shown for both gravity and simulated microgravity conditions in Figure 4.4. The biofilms that accumulated on the tube walls were over five times greater, on average, in the gravity condition which coincides with the cells only settling during the experiment. Since the cells for the simulated microgravity condition are calculated to be in constant suspension, the comparatively low formation of biofilms within the tube further validates those calculations.

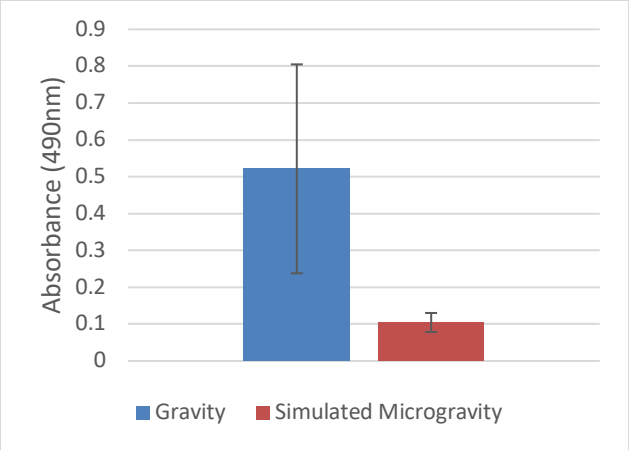

Figure 4.4 Biofilm formation based on treatment group of *E. coli* after being on the clinostat for 24 hours.

The treatment and control samples had been subjected to another 24 hours of growth in static conditions to view persistent changes in biofilm formation after exposure to simulated microgravity. Figure 4.5 shows that the treatment group formed up to three times the quantity of biofilms compared to the control group. Past literature has shown that microgravity conditions tend to enhance the formation of biofilms (McLean et al., 2001; Lynch et al., 2006)

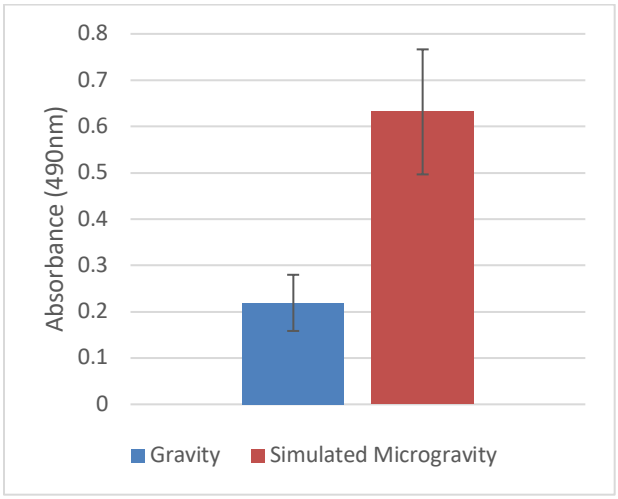

Figure 4.5 Biofilm formation based on treatment group of *E. coli* 24 hours after being on the clinostat for 24 hours.

4.3 Differential Gene Analysis

With the biofilm experiment providing an increase in biofilm formation for the treatment group following growth after simulated microgravity, RNA samples were sequenced to view changes in gene regulation (Castillo et al., unpublished). Figures 4.6 and 4.7 show the categories of gene biological processes that were up or down regulated under microgravity, respectively. These figures utilized a REVIGO plotting method where clusters that are closer to one another have similar biological processes (Supek et al., 2011). Additionally, the color intensity reflects the frequency of regulation for that biological process (Supek et al., 2011). Of the categories that were up regulated, four were directly related to biofilm formation: biological adhesion, cell aggregation, single-species biofilm formation, cell adhesion and cell motility. This knowledge verifies the biofilm results were correct in that biofilm formation had indeed increased due to simulated microgravity. Of the gene biological processes that were down regulated, multiple were in relation to aerobic conditions: ATP metabolic process and energy derivation by oxidation of organic compounds. Since the tubes did not have gas exchange capabilities, the cells would have undergone anaerobic growth. Without the need to grow aerobically, it is warranted that *E. coli* would reduce the regulation of these genes.

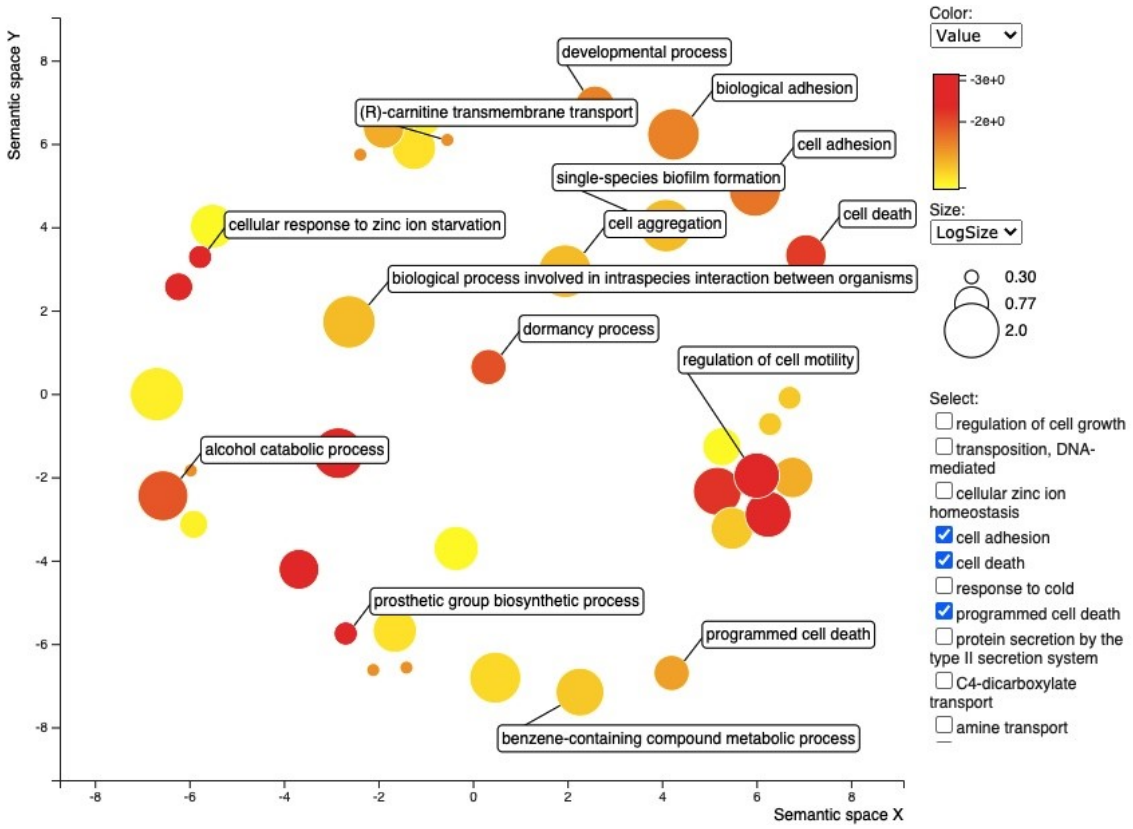

Figure 4.6 Up regulated gene biological processes based on treatment group of *E. coli* 24 hours after being on the clinostat for 24 hours.

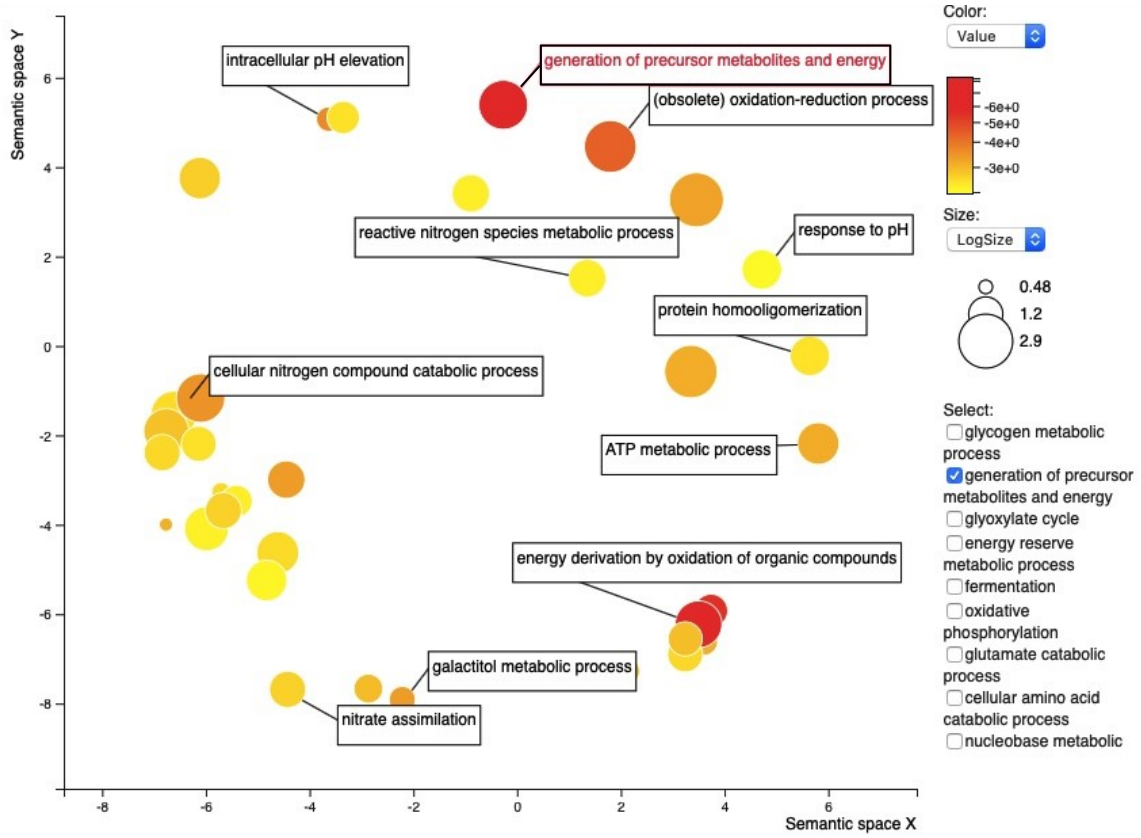

Figure 4.7 Down regulated gene biological processes based on treatment group of *E. coli* 24 hours after being on the clinostat for 24 hours.

4.4 CFD Results

4.4.1 Mesh Independence

The mesh independence study (Table 4.1) completed 50 iterations for each trial and the element size from Trial 7 was chosen to complete all simulations with because both weighted average values were under 1% different from the next size down. Trial 5 also met this criterion, however, there was only a 19.6% increase in elements for the following trial whereas Trial 7 to 8 had a 66.6%

element increase. Due to this, Trial 7 was taken to be more reliable, and a final mesh is provided in Figure 4.8.

Table 4.1 Mesh Independence Study using Case 1 – Gravity.

Trial	Mesh Element Size (m)	Mesh Nodes	Mesh Elements	Area-Weighted Average	Percent Difference	Volume-Weighted Average	Percent Difference
1	0.005	51992	49152	0.01125	N/A	0.011121	N/A
2	0.001	52574	49728	0.011556	2.68%	0.011387	2.36%
3	0.0005	65863	62592	0.011404	1.32%	0.011216	1.51%
4	0.0004	75175	71904	0.01116	2.16%	0.011204	0.11%
5	0.0003	77503	74016	0.010948	1.92%	0.011085	1.07%
6	0.0002	93896	90144	0.010906	0.38%	0.011046	0.35%
7	0.00015	130660	127100	0.011376	4.22%	0.01126	1.92%
8	0.0001	258310	254020	0.011278	0.87%	0.011222	0.34%
9	0.00005	711790	704450	0.011539	2.29%	0.011467	2.16%

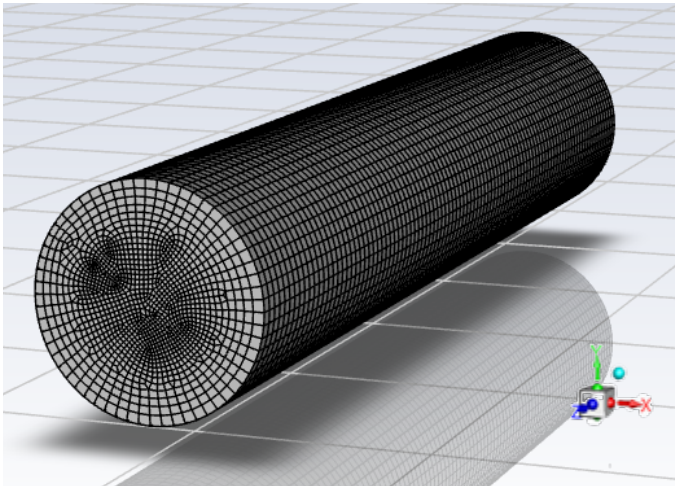

Figure 4.8 Mesh used throughout all simulations.

4.4.2 Case 1 – Gravity

From the final mesh, the simulation was completed to visualize the steady-state concentration of cells, see Figure 4.9. The volume fraction of *E. coli* that was initially 1% throughout the vessel now has a 5.39% along the bottom while much of the tube has under 1%. Given that gravity was added in only the negative y-

direction, the bacteria should have settled towards the bottom making this first case successful. This case was also validated experimentally using *A. platensis* on the clinostat to easily visualize the case. In Figure 4.10, this demonstration is shown, and the cyanobacteria have settled on the bottom of the tubes.

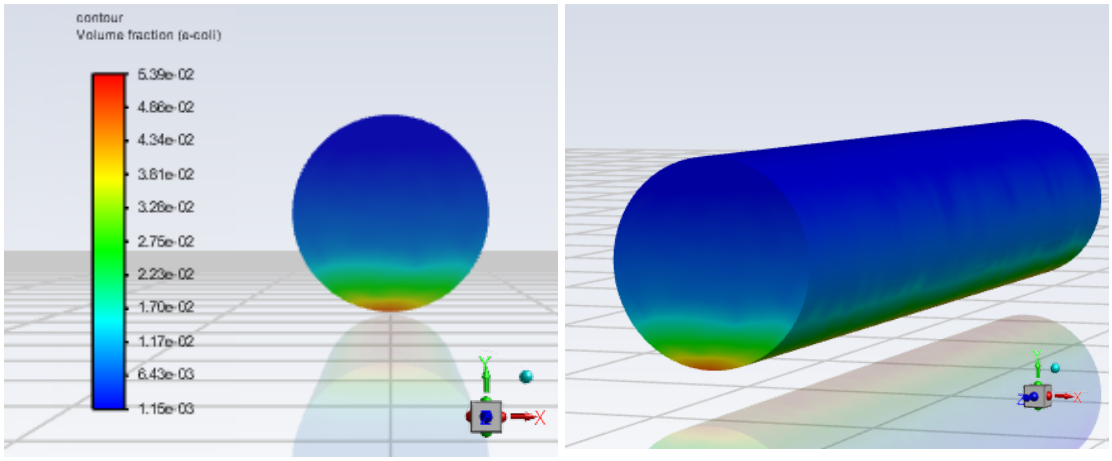

Figure 4.9 Simulation of Case 1 with only gravity enabled.

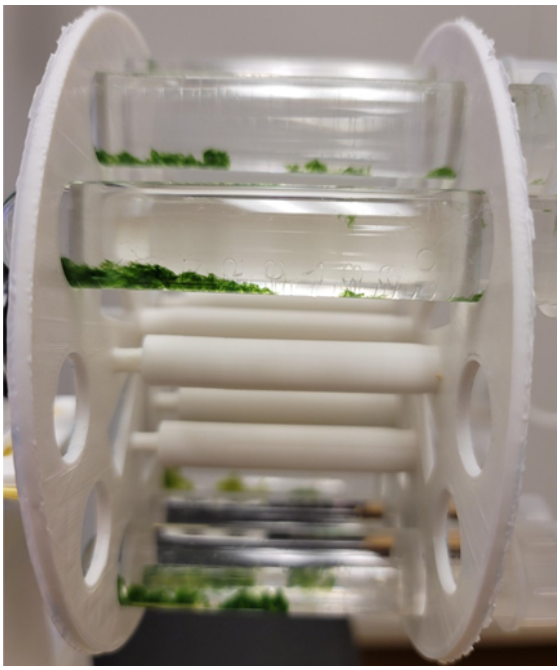

Figure 4.10 Experimental demonstration without rotation on the clinostat using *A. platensis*.

4.4.3 Simulating Growth

To simulate the bacteria growth for cases two and three, the experimental growth rate found from Figure 4.2 was incorporated as a Mass Source term for *E. coli* using Fluent's expression editor. The term was initially in cells generated per hour which was converted to cells per second. Another factor was modeling the growth based on the concentration of bacteria throughout the container. Since bacteria generation is not uniform through the tube, the growth rate was multiplied by the ratio of the volume fraction of *E. coli* in an element compared to the maximum volume fraction of *E. coli* from the previous iteration. This would generate less bacteria when less is present. Equation 4.1 was created to define the growth rate based on these parameters. From Figure 4.2, the bacteria are in their exponential phase between the two and seven hours, so growth was only permitted during these times.

$$Growth\ Rate = \frac{12335\ [\frac{cells}{s}] * m_{cell}}{V_{tube}} * \frac{V_{frac}}{V_{frac\_max}} \tag{4.1}$$

4.4.4 Case 2 – Rapid Rotation

Building from case one, the clinostat rotation was included in the gravity terms. The intention for the second trial was to demonstrate the effects of rotating too quickly which would force the bacteria against the wall furthest from the rotation axis. This problem used 100 RPM without growth, initially, and after the 24-hour period a gradient similar to the gravity-only case, but in the opposite

direction, was found. As shown in Figure 11, instead of the cells settling to the bottom the cells were forced towards the top of the tube. Next, the growth rate was incorporated resulting in a slightly modified result, Figure 4.12, but still maintaining the same distribution as the previous trial. Case two was also verified using *A. platensis*, shown in Figure 13, which demonstrates the cells forced against the outer wall of the tube. Additionally, this figure was modified to make the tube wall more visible.

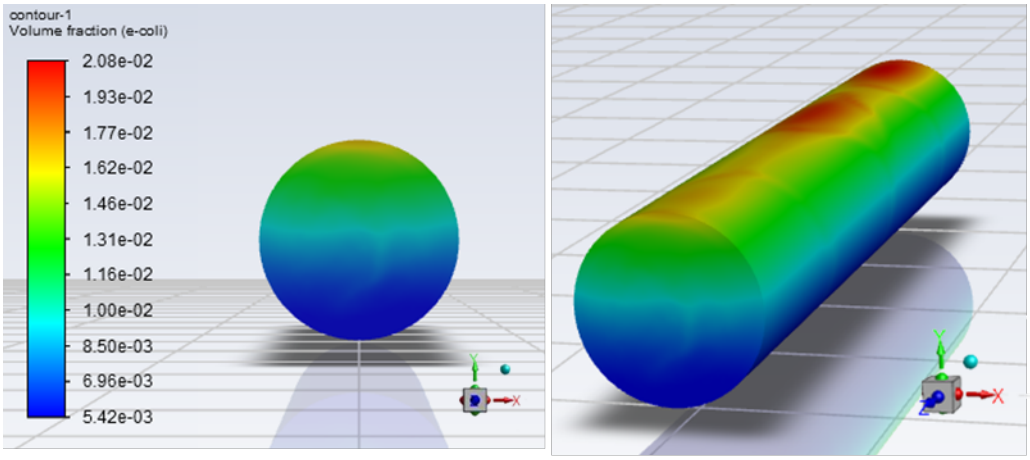

Figure 4.11 Simulation of 100 RPM speed without bacteria growth.

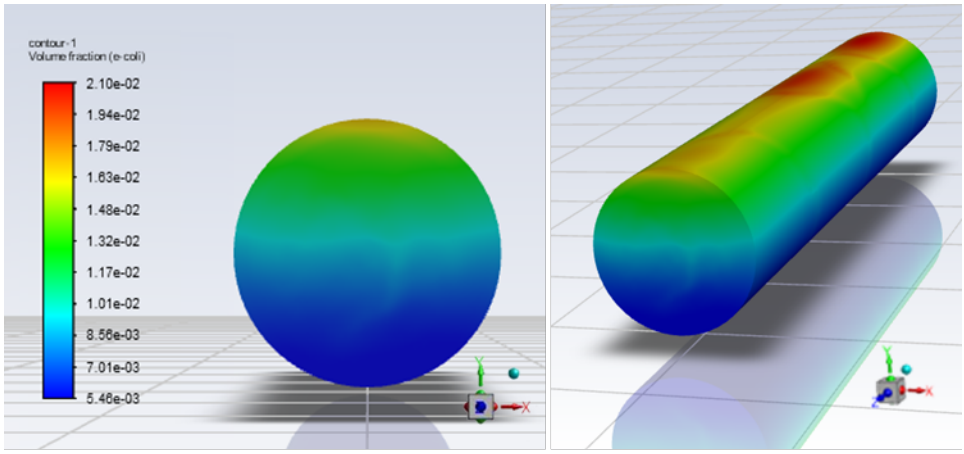

Figure 4.12 Simulation of 100 RPM speed that includes bacteria growth.

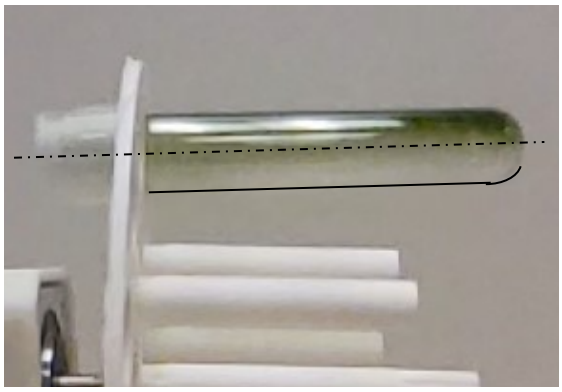

Figure 4.13 Experimental demonstration with 100 RPM rotation on the clinostat using *A. platensis*.

4.4.5 Case 3 – Simulated Microgravity

The final case was the 8 RPM that was shown to be capable of providing functional weightlessness, in Section 3.2.2, for the bacteria. Two subcases were necessary to consider, which were with and without growth. The non-growth trial provided a baseline for the cell fraction distribution to understand any changes resulting from growth. Figure 4.14 shows the non-growth result after the 24-hour period. This result clearly demonstrates the gradient of concentration that was impacted by the centrifugal acceleration term. However, once the growth rate was applied, see Figure 4.15, the distribution of cells varied by only 1.96% throughout. Along with this, the experimental demonstration using *A. platensis* also shows the nearly even bacteria distribution with some tubes having small aggregations forming.

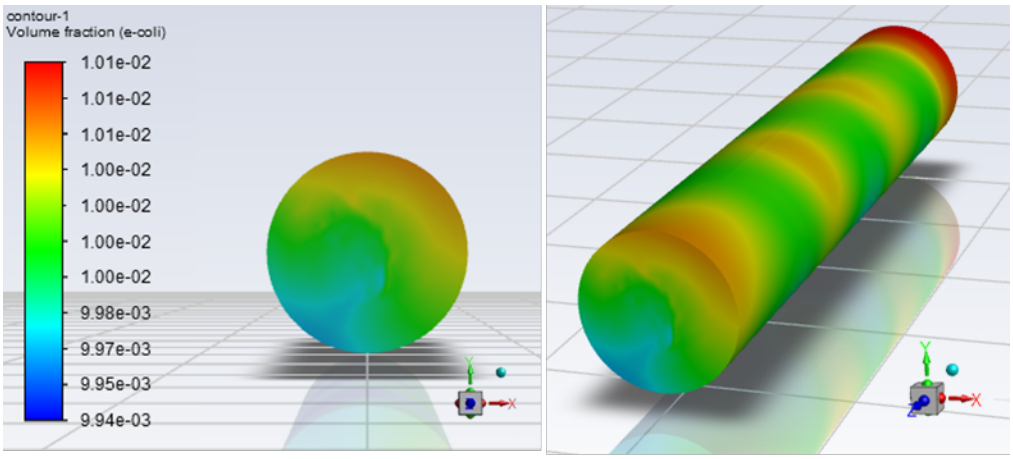

Figure 4.14 Simulation of 8RPM speed without bacteria growth.

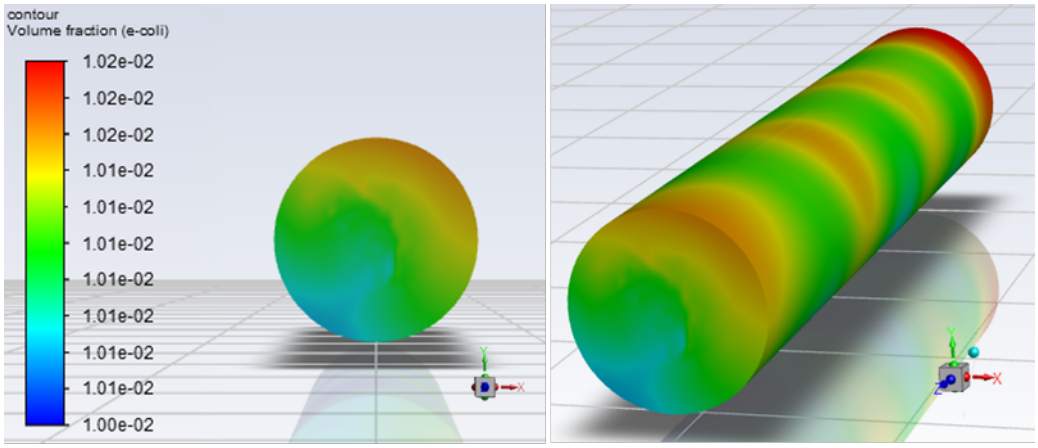

Figure 4.15 Simulation of 8RPM speed that includes bacteria growth.

Figure 4.16 Experimental demonstration with 8 RPM rotation on the clinostat using *A. platensis*.

4.6 Prototype Vessels

One of the tubes that had a membrane had leaked during the 72-hour period so only the one sample was used to compare with the two that did not have a membrane. After the 72 hours, the two vessels with only media inside were verified to be free of contamination. The other prototype vessels were then mixed via a pipette and measured for optical density. As shown in Figure 4.17, there was 70% more growth that occurred for the sample with the membrane compared to without the membrane. This result aligns with previous knowledge that facultative organisms show enhanced growth in the presence of oxygen (Tortora, Funke & Case, 2013).

Figure 4.17 Optical density values for *E. coli* grown in the prototype vessels.

Although the membrane sample was determined to have enhanced growth, the tube design can be compared with the growth curve from the clinostat experiment to improve the design. Because there is zero headspace in the tubes, the bacteria can only encounter oxygen from diffusion through the membrane. Given that diffusion will be symmetrical, only half of the tube is considered since the cells at that point will be most reliant on the diffusion. Thus, the consumption rate for *E. coli* compared to the availability of oxygen must be understood.

The Breathe-Easy membrane used has an oxygen exchange rate of $553.5\frac{mL}{24hr*in^2}$ (or $9.9 * 10^{-6}\frac{mL}{s*cm^2}$) as provided by the specifications sheet (*Research Products International*). The area of membrane used was $1.13cm^2$ on each side of the tube. By multiplying the area with the exchange rate, this provides an oxygen exchange rate of $1.122 * 10^{-5}\frac{mL}{s}$ from one side. With standard atmospheric pressure and a temperature of

37°C, the ideal gas law equation can estimate the available moles per second of oxygen, see Eq 4.2.

$$n = \frac{PV}{RT} = \frac{1[atm]*1.122*10^{-5}[\frac{mL}{s}]}{0.08206[\frac{L*atm}{mol*K}]*310.15[K]} = 4.409 * 10^{-7}[\frac{mol_{O_2}}{hr}] \quad (4.2)$$

where n is number of moles, P is atmospheric pressure, V is volume, R is the ideal gas constant and T is temperature.

Past research has shown that *E. coli* consumes less than $0.015\frac{mol}{g*hr}$ of oxygen (Calhoun et al., 1993). From the clinostat experiment, the largest amount of cells was $2.42 * 10^8$ for a mass of $2.42 * 10^{-4}g$ which gives a maximum consumption rate of $3.63 * 10^{-6}\,\frac{mol_{O_2}}{hr}$. Compared with the available oxygen, there is 30 times less than the required amount to keep *E. coli* in respiration. However, this availability only occurs immediately at the membrane interface and the worst case is being observed. From membrane interface to the center of the tube, the diffusion of oxygen must go through the media which will be a slower process.

With the assumption of the media being water and at 37°C, the diffusion coefficient of oxygen was estimated to be $2.75 * 10^{-5}[\frac{cm^2}{s}]$ (Yin & Zhang, 2014). Applying this value in Eq. 2.4.7 and solving for time gives the plot shown in Figure 4.18.

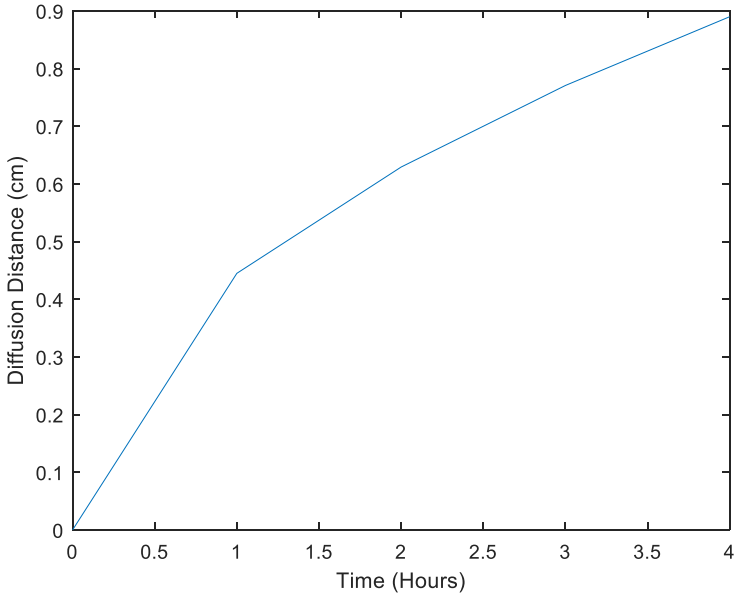

Figure 4.18 Diffusion of oxygen through the prototype vessel.

Based on this data, the oxygen will diffuse through the media and reach the midpoint of the tube (0.83 cm) after 3.5 hours. If the bacteria at this center region exhaust the soluble oxygen before additional oxygen has diffused through the media, then the cells will begin to ferment. This would result in an unbalanced growth dynamic if both types of growth are occurring.

Looking at .25 cm on both sides of the tube midpoint and assuming the homogeneous distribution of cells throughout the experiment can determine if this event will occur. With 3.5 hours until additional oxygen supplementation, the cell count at the first timepoint was used. Additionally, the volume fraction being looked at would be 0.5 cm over the vessel length, 1.66 cm, or 0.30. The consumption rate for 30% of cells initially placed on the clinostat was $3.4 * 10^{-7}[\frac{mol_{O_2}}{hr}]$.

Now, the expected amount of soluble oxygen in the media at 37°C was found to be 6.8602$\frac{mg}{L}$ or $2.1438 * 10^{-4}\,\frac{mol_{O_2}}{L}$ based on data from Truesdale, Downing & Lowden. Given the vessels created were 2 mL and looking at 30% of the total value, this provides $1.2861 * 10^{-7} mol_{O_2}$ available within the center region. The consumption rate in this center region is more than 2.5 times the soluble oxygen. Therefore, these cells will have begun fermentation after roughly twenty minutes until oxygen has diffused.

Based on these findings, the current vessel design does not allow enough oxygen to be delivered to prevent fermentation from occurring. Any subsequent vessels that are created should prevent this difference in growth dynamics. The main solution to this issue is to construct the vessel with a larger radius to length ratio. Alternatively, it would prove beneficial to position the membrane along the length of the vessel versus the ends to provide a more equal diffusion of oxygen through the vessel. Otherwise, a membrane with a much higher oxygen permeability would be desirable.

5. Conclusions and Recommendations

5.1 Conclusions

This research aimed to create and validate a low shear simulated microgravity analog specific for bacterial growth. The instrument was subjected to requirements imposed by literature, experimental comparison with an industry standard device, biofilm analysis, and computation fluids dynamics. All methods provided results showing the clinostat was indeed capable of created the simulated microgravity environment. Based on literature, the unit was deemed to provide functional weightlessness while maintain a relatively low centrifugal acceleration value. Cell concentration of *E. coli* after 24 hours was greater in the simulated microgravity condition compared to the control which agreed with the RCCS result and past experiments. Biofilm formation for these cells had been greater after being cultured following the clinostat experiment which was verified by the up regulation in gene expression found. Additionally, this research developed prototype gas exchange vessels to specifically grow aerobic bacteria. Now that the platform has been verified to function as intended, there are many avenues to continue the research further.

5.2 Future Research / Recommendations

The greatest determinant of simulating microgravity would be validating the device with an experiment in space. However, in space, the two environmental variables are microgravity and radiation. To properly isolate the effects of microgravity, additional testing is required that includes using different prokaryotic and eukaryotic models that

require the adjustment of the rotational speed. The CFD simulation can be further improved by increasing the fidelity of the growth curve used for any organism as well as modeling gas exchange to computationally validate the O_2 and CO_2 concentrations. This gas modeling should also be validated experimentally with gas tracking sensors. Another factor to consider based on the microorganism used would be the optimization of the RPM throughout the experiment. Given that some bacteria will have a large change in mass, it is possible that a profile will need to be created to automatically adjust the RPM.

5.3 Broader Impact

With the designed clinostat capable of completing whole experiments quickly at a relatively low build cost, completing research can become more accessible for other scientists and university or high school students. Doing so will allow microgravity studies to become more common and greatly expand on the current research that is out there. Currently, the clinostat has been incorporated into multiple undergraduate microbiology-related courses at Embry-Riddle Aeronautical University.

References

Abomohra, A. E. F., El-Shouny, W., Sharaf, M., & Abo-Eleneen, M. (2016). Effect of gamma radiation on growth and metabolic activities of Arthrospira platensis. Brazilian Archives of Biology and Technology, 59.

Ali, S. K., & Saleh, A. M. (2012). Spirulina-an overview. International journal of Pharmacy and Pharmaceutical sciences, 4(3), 9-15.

Arunasri, K., Adil, M., Charan, K. V., Suvro, C., Reddy, S. H., & Shivaji, S. (2013). Effect of simulated microgravity on E. coli K12 MG1655 growth and gene expression. *PloS one*, *8*(3), e57860.

Asghari, A., Fazilati, M., Latifi, A. M., Salavati, H., & Choopani, A. (2016). A review on antioxidant properties of Spirulina. *Journal of Applied Biotechnology Reports*, *3*(1), 345-351.

Aunins, T. R., Erickson, K. E., Prasad, N., Levy, S. E., Jones, A., Shrestha, S., ... & Chatterjee, A. (2018). Spaceflight modifies Escherichia coli gene expression in response to antibiotic exposure and reveals role of oxidative stress response. *Frontiers in microbiology*, *9*, 310.

Autoclavable HARV Spec Sheet. (n.d.). In *Synthecon*. Retrieved from https://synthecon.com/pages/synthecon_autoclavable_high_aspect_ratio_vessels_27.asp

Böhmer, M., & Schleiff, E. (2019). Microgravity research in plants. *EMBO Reports*, 20(7), e48541. https://doi.org/10.15252/embr.201948541

Brown, R. B. (1999). *Effects of Space Flight, Clinorotation, and Centrifugation on the Growth and Metabolism of Escherichia coli*. COLORADO UNIV AT BOULDER.

Brungs, S., Hauslage, J., & Hemmersbach, R. (2019). Validation of Random Positioning Versus Clinorotation Using a Macrophage Model System. *Microgravity Science and Technology, 31*(2), 223–230. https://doi.org/10.1007/s12217-019-9687-0

Calhoun, M. W., Oden, K. L., Gennis, R. B., de Mattos, M. J., & Neijssel, O. M. (1993). Energetic efficiency of Escherichia coli: Effects of mutations in components of the aerobic respiratory chain. Journal of Bacteriology, 175(10), 3020–3025.

Capelli, B., & Cysewski, G. R. (2010). Potential health benefits of spirulina microalgae. Nutrafoods, 9(2), 19-26.

Castillo, H., Li, X., Schilkey, F., & Smith, G. B. (2018). Transcriptome analysis reveals a stress response of *Shewanella oneidensis* deprived of background levels of ionizing radiation. *PloS one*, *13*(5), e0196472.

Chavez-Dozal, A. A., Nourabadi, N., Erken, M., McDougald, D., & Nishiguchi, M. K. (2016). Comparative analysis of quantitative methodologies for Vibrionaceae biofilms. *Folia microbiologica, 61*(6), 449-453.

Chen, Y. H., Chang, G. K., Kuo, S. M., Huang, S. Y., Hu, I. C., Lo, Y. L., & Shih, S. R. (2016). Well-tolerated Spirulina extract inhibits influenza virus replication and reduces virus-induced mortality. Scientific reports, 6(1), 1-11.

Ciferri, O. (1983). Spirulina, the edible microorganism. *Microbiological Reviews*, *47*(4), 551–578. https://doi.org/10.1128/MMBR.47.4.551-578.1983

Costerton, J. W., Lewandowski, Z., Caldwell, D. E., Korber, D. R., & Lappin-Scott, H. M. (1995). Microbial biofilms. *Annual review of microbiology, 49*(1), 711-745.

Dillon, J. C., Phuc, A. P., & Dubacq, J. P. (1995). Nutritional Value of the Alga Spirulina. In A. P. Simopoulos (Ed.), World Review of Nutrition and Dietetics (Vol. 77, pp. 32–46). S. Karger AG. https://doi.org/10.1159/000424464

Dineshkumar R, Narendran R, Sampathkumar P. () Cultivation of Spirulina platensis in different selective media. *Indian Journal of Geo-Marine Sciences*, *45*(12):1749-1754.

Doyle, M. P., & Schoeni, J. L. (1984). Survival and growth characteristics of Escherichia coli associated with hemorrhagic colitis. *Applied and Environmental Microbiology*, *48*(4), 855-856.

Eckart, P. (1996). Spaceflight Life Support and Biospherics. Springer Netherlands. https://public.ebookcentral.proquest.com/choice/publicfullrecord.aspx?p=5590958

Feng, D. L., & Wu, Z. C. (2006). Culture of Spirulina platensis in human urine for biomass production and O 2 evolution. Journal of Zhejiang University Science B, 7(1), 34-37.

Garrity, G. M., Bell, J. A., & Lilburn, T. G. (2004). Taxonomic outline of the prokaryotes. Bergey's manual of systematic bacteriology. Springer, New York, Berlin, Heidelberg.

Hayashi, T., Hayashi, K., Maeda, M., & Kojima, I. (1996). Calcium spirulan, an inhibitor of enveloped virus replication, from a blue-green alga Spirulina platensis. Journal of natural products, 59(1), 83-87.

Hendrickx, L., De Wever, H., Hermans, V., Mastroleo, F., Morin, N., Wilmotte, A., ... & Mergeay, M. (2006). Microbial ecology of the closed artificial ecosystem MELiSSA (Micro-Ecological Life Support System Alternative): reinventing and compartmentalizing the Earth's food and oxygen regeneration system for long-haul space exploration missions. Research in microbiology, 157(1), 77-86.

Herranz, R., Anken, R., Boonstra, J., Braun, M., Christianen, P. C. M., de Geest, M., Hauslage, J., Hilbig, R., Hill, R. J. A., Lebert, M., Medina, F. J., Vagt, N., Ullrich, O., van Loon, J. J. W. A., & Hemmersbach, R. (2013). Ground-Based Facilities for Simulation of Microgravity: Organism-Specific Recommendations for Their Use, and Recommended Terminology. *Astrobiology*, 13(1), 1–17. https://doi.org/10.1089/ast.2012.0876

Hou, X., Lu, Y., Zhang, Z., & Wang, W. (2009). The breeding of Arthrospira platensis mutants with good quality and high yield induced by space flight. *Induced Plant Mutations in the Genomics Era*, 293-295.

Idalia, V.-M. N., & Bernardo, F. (2017). Escherichia coli as a Model Organism and Its Application in Biotechnology. In A. Samie (Ed.), Escherichia coli—Recent Advances on Physiology, Pathogenesis and Biotechnological Applications. InTech. https://doi.org/10.5772/67306

Jones, H. W. (2015). The Life Cycle Cost (LCC) of Life Support Recycling and Resupply. *45th International Conference on Environmental Systems.* https://ntrs.nasa.gov/search.jsp?R=20160001262

Jones, H. W., Hodgson, E. W., Gentry, G. J., & Kliss, M. H. (2016). How Do Lessons Learned on the International Space Station (ISS) Help Plan Life Support for Mars? *46th International Conference on Environmental Systems.* https://ntrs.nasa.gov/search.jsp?R=20160014540

Karkos, P. D., Leong, S. C., Karkos, C. D., Sivaji, N., & Assimakopoulos, D. A. (2011). Spirulina in clinical practice: evidence-based human applications. Evidence-based complementary and alternative medicine, 2011.

Kacena, M. A., Merrell, G. A., Manfredi, B., Smith, E. E., Klaus, D. M., & Todd, P. (1999). Bacterial growth in space flight: Logistic growth curve parameters for Escherichia coli and Bacillus subtilis. *Applied Microbiology and Biotechnology, 51*(2), 229–234. https://doi.org/10.1007/s002530051386

Klaus, D., Luttges, M., & Stodieck, L. (1994). Investigation of Space Flight Effects on Escherichia coli Growth. *SAE Transactions, 103*, 470-478. Retrieved March 25, 2021, from http://www.jstor.org/stable/44614859

Klaus, D., Simske, S., Todd, P., & Stodieck, L. (1997). Investigation of space flight effects on Escherichia coli and a proposed model of underlying physical mechanisms. *Microbiology*, 143(2), 449–455. https://doi.org/10.1099/00221287-143-2-449

Klaus, D. M., Todd, P., & Schatz, A. (1998). Functional weightlessness during clinorotation of cell suspensions. *Advances in Space Research*, *21*(8–9), 1315–1318. https://doi.org/10.1016/S0273-1177(97)00404-3

Klaus, D. M. (2001). Clinostats and bioreactors. *Gravitational and Space Biology Bulletin: Publication of the American Society for Gravitational and Space Biology*, *14*(2), 55–64.

Krauss, H. L., Bostian, C. W., & Raab, F. H. (2013). Teacher's Guide to Plant Experiments in Microgravity. *New York: United Nations*.

Leys, N. (2018). *Arthrospira-B* First photobioreactor for oxygen and edible biomass production in space. *MELiSSA Foundation Conference in Rome* https://www.melissafoundation.org/page/roma

Lynch, S. V., Mukundakrishnan, K., Benoit, M. R., Ayyaswamy, P. S., & Matin, A. (2006). Escherichia coli Biofilms Formed under Low-Shear Modeled Microgravity in a Ground-Based System. Applied and Environmental Microbiology, 72(12), 7701–7710. https://doi.org/10.1128/AEM.01294-06

Makhlouf, R., & Makhlouf, I. (2012). Evaluation of the effect of Spirulina against Gamma irradiation induced oxidative stress and tissue injury in rats. *International Journal of Applied Science and Engineering Research*, 1(1), 152-164.

Matin, A., & Lynch, S. V. (2005). Investigating the threat of bacteria grown in space. *ASM News*, *71*(5), 235-240.

McLean, R. J. C., Cassanto, J. M., Barnes, M. B., & Koo, J. H. (2001). Bacterial biofilm formation under microgravity conditions. *FEMS Microbiology Letters*, 195(2), 115–119. https://doi.org/10.1111/j.1574-6968.2001.tb10507.x

Mika, J. T., Thompson, A. J., Dent, M. R., Brooks, N. J., Michiels, J., Hofkens, J., & Kuimova, M. K. (2016). Measuring the viscosity of the Escherichia coli plasma membrane using molecular rotors. *Biophysical journal*, *111*(7), 1528-1540.

Moro-Aguilar, R. (2014). The New Commercial Suborbital Vehicles: An Opportunity for Scientific and Microgravity Research. *Microgravity Science and Technology, 26*(4), 219–227. https://doi.org/10.1007/s12217-014-9378-9

Nickerson, C. A., Ott, C. M., Wilson, J. W., Ramamurthy, R., & Pierson, D. L. (2004). Microbial responses to microgravity and other low-shear environments. *Microbiology and Molecular Biology Reviews*, *68*(2), 345-361.

Niederwieser, T., Kociolek, P., & Klaus, D. (2018). A review of algal research in space. *Acta Astronautica*, *146*, 359–367. https://doi.org/10.1016/j.actaastro.2018.03.026

Patnaik, R., & Liao, J. C. (1994). Engineering of Escherichia coli central metabolism for aromatic metabolite production with near theoretical yield. *Applied and Environmental Microbiology*, *60*(11), 3903-3908.

Poughon, L., Laroche, C., Creuly, C., Dussap, C. G., Paille, C., Lasseur, C., ... & Leys, N. (2020). Limnospira indica PCC8005 growth in photobioreactor: model and simulation of the ISS and ground experiments. *Life sciences in space research, 25*, 53-65.

Rajagopal, S. S. D. S. M., Murthy, S. D. S., & Mohanty, P. (2000). Effect of ultraviolet-B radiation on intact cells of the cyanobacterium Spirulina platensis: characterization of the alterations in the thylakoid membranes. *Journal of Photochemistry and Photobiology B: Biology*, 54(1), 61-66.

Rice, J. C., Peng, T., Spence, J. S., Wang, H. Q., Goldblum, R. M., Corthésy, B., & Nowicki, B. J. (2005). Pyelonephritic Escherichia coli expressing P fimbriae decrease immune response of the mouse kidney. *Journal of the American Society of Nephrology*, 16(12), 3583-3591.

Supek, F., Bošnjak, M., Škunca, N., & Šmuc, T. (2011). REVIGO summarizes and visualizes long lists of gene ontology terms. *PloS one*, *6*(7), e21800.

Ratiu, I.-A., Ligor, T., Bocos-Bintintan, V., Al-Suod, H., Kowalkowski, T., Rafińska, K., & Buszewski, B. (2017). The effect of growth medium on an Escherichia coli pathway mirrored into GC/MS profiles. *Journal of Breath Research*, *11*(3), 036012. https://doi.org/10.1088/1752-7163/aa7ba2

Sili, C., Torzillo, G., & Vonshak, A. (2012). Arthrospira (Spirulina). In Ecology of cyanobacteria II (pp. 677-705). Springer, Dordrecht.

Storrs-Mabilat, M. (2001). Study of a microbial detection system for space applications. In *Second Workshop on Advanced Life Support*, Noordwijk, The Netherlands.

Sukumaran, P., Nulit, R., Halimoon, N., Simoh, S., Omar, H., & Ismail, A. (2018). formulation of cost-effective medium using urea as a nitrogen source for Arthrospira platensis cultivation under real environment. *Annual Research & Review in Biology*, 1-12.

"Technical Data Sheet Breathe-Easy™ Sealing Membrane." *Research Products International*, d2gdaxkudte5p.cloudfront.net/system/product_documents/TDS%20248738.pdf.

Thévenet, D., D'ari, R., & Bouloc, P. (1996). The SIGNAL experiment in BIORACK: Escherichia coli in microgravity. *Journal of biotechnology*, *47*(2-3), 89-97.

Thomas, V., Prasad, N., & Reddy, C. (2000). Microgravity research platforms – A study. *Current Science, 79*(3), 336-340.

Todd, P. (1989). Gravity-Dependent Phenomena at the Scale of the Single Cell. *Gravitational and Space Research*, 2(1), Article 1. http://gravitationalandspaceresearch.org/index.php/journal/article/view/58

Tortora, G. J., Funke, B. R., & Case, C. L. (2013). *Microbiology: An introduction.*

Truesdale, G. A., Downing, A. L., & Lowden, G. F. (1955). The solubility of oxygen in pure water and sea-water. *Journal of Applied Chemistry*, *5*(2), 53-62.

United Nations World Food Conference (1974) As reported on the Intergovernmental Institution for the Use of Microalgae Spirulina Against Malnutrition (Permanent Observer to the United Nations Economic and Social Council) www.iimsam.org

Vukanti, R., Mintz, E., & Leff, L. (2008). Changes in gene expression of E. coli under conditions of modeled reduced gravity. Microgravity-Science and Technology, 20(1), 41-57.

Wagner, E. B., Charles, J. B., & Cuttino, C. M. (2009). Opportunities for research in space life sciences aboard commercial suborbital flights. Aviation, space, and environmental medicine, 80(11), 984-986.

Wilson, J. W., Ott, C. M., Zu Bentrup, K. H., Ramamurthy, R., Quick, L., Porwollik, S., ... & Nickerson, C. A. (2007). Space flight alters bacterial gene expression and virulence and reveals a role for global regulator Hfq. *Proceedings of the National Academy of Sciences*, *104*(41), 16299-16304.

Yin, G., & Zhang, J. (2014). *Rotating electrode methods and oxygen reduction electrocatalysts*. Elsevier.

Zea, L., Larsen, M., Estante, F., Qvortrup, K., Moeller, R., Dias de Oliveira, S., ... & Klaus, D. (2017). Phenotypic changes exhibited by E. coli cultured in space. *Frontiers in microbiology*, *8*, 1598.

Zea, L., McLean, R. J. C., Rook, T. A., Angle, G., Carter, D. L., Delegard, A., Denvir, A., Gerlach, R., Gorti, S., McIlwaine, D., Nur, M., Peyton, B. M., Stewart, P. S., Sturman, P., & Velez Justiniano, Y. A. (2020). Potential biofilm control strategies for extended spaceflight missions. *Biofilm, 2*, 100026. https://doi.org/10.1016/j.bioflm.2020.100026